

## Article

# Health Impact Assessment of Air Pollution under a Climate Change Scenario: Methodology and Case Study Application

Sílvia Coelho <sup>1</sup>, Joana Ferreira <sup>1,\*</sup>, David Carvalho <sup>2</sup> and Myriam Lopes <sup>1</sup><sup>1</sup> CESAM & Department of Environment and Planning, University of Aveiro, 3810-193 Aveiro, Portugal<sup>2</sup> CESAM & Department of Physics, University of Aveiro, 3810-193 Aveiro, Portugal

\* Correspondence: jferreira@ua.pt

**Abstract:** The World Health Organization estimates that every year air pollution kills seven million people worldwide. As it is expected that climate change will affect future air quality patterns, the full understanding of the links between air pollution and climate change, and how they affect human health, are challenges for future research. In this scope, a methodology to assess the air quality impacts on health was developed. The WRF-CAMx modelling framework was applied for the medium-term future climate (considering the SSP2-4.5 scenario) and for the recent past (considered as baseline). Following the WHO recommendations, mortality health indicators were used to estimate the health impacts of long-term exposures. For that, the Aveiro Region, in Portugal, was considered as a case study. Future climate results indicate the occurrence of higher temperatures, and lower total precipitation. Despite that, improvements in the main pollutants' concentrations, and consequently in the reduction of the related premature deaths are foreseen, mainly due to the reduction of pollutants emissions imposed by the European legislation for the upcoming years. The applied approach constitutes an added value in this research field, being crucial to anticipate the effects of climate change on air quality and evaluate their impacts on human health.

**Keywords:** SSP (Shared Socio-economic Pathway) scenarios; air quality; WRF-CAMx; numerical modelling; urban areas; health impact assessment; premature deaths



check for updates

**Citation:** Coelho, S.; Ferreira, J.; Carvalho, D.; Lopes, M. Health Impact Assessment of Air Pollution under a Climate Change Scenario: Methodology and Case Study Application. *Sustainability* **2022**, *14*, 14309. <https://doi.org/10.3390/su142114309>

Academic Editor: Pallav Purohit

Received: 13 September 2022

Accepted: 31 October 2022

Published: 2 November 2022

**Publisher's Note:** MDPI stays neutral with regard to jurisdictional claims in published maps and institutional affiliations.



**Copyright:** © 2022 by the authors. Licensee MDPI, Basel, Switzerland. This article is an open access article distributed under the terms and conditions of the Creative Commons Attribution (CC BY) license (<https://creativecommons.org/licenses/by/4.0/>).

## 1. Introduction

Nowadays, air pollution and climate change are two of the biggest environmental and health threats, with increasing concern among people worldwide [1], being expected to continue for the next decades [2]. More than 70% of the European Union (EU) population live in urban areas [3], where economic activities cause high levels of air pollution [4]. Citizens' exposure to air pollutants, like particulate matter with a diameter of 10 microns or less (PM<sub>10</sub>) and with a diameter of 2.5 microns or less (PM<sub>2.5</sub>), nitrogen dioxide (NO<sub>2</sub>), and ozone (O<sub>3</sub>), has been threatening human health. The EU Air Quality Directive (Directive 2008/50/EC [5]) aims to protect health, vegetation, and natural ecosystems, through the definition of limit and target values for those air pollutants, among others. In 2020, less than 1% of the EU urban population lived in zones with PM<sub>2.5</sub> and NO<sub>2</sub> concentrations above the EU limit values, while 12% of citizens were exposed to O<sub>3</sub>, and 11% to PM<sub>10</sub> levels above EU standards [4]. However, when considering the new 2021 World Health Organization (WHO) air quality recommendations [6], in 2020, the EU urban population exposure raised to 96% for PM<sub>2.5</sub>, 89% for NO<sub>2</sub>, 71% for PM<sub>10</sub>, and 93% for O<sub>3</sub> [4]. These data have become more relevant since the EU Clean Air Programme [7] and the European Green Deal [8] proposed a revision of the ambient air quality directives, aiming to closely align the EU air quality standards with the WHO recommendations [4]. The WHO estimates that every year, ambient air pollution kills around 4.2 million people worldwide, due to stroke, heart disease, lung cancer, lower respiratory infections, and chronic obstructive pulmonary disease [9]. In 2019, in the EU alone, the estimated premature deaths attributable

to long-term exposure to PM<sub>2.5</sub>, NO<sub>2</sub>, and O<sub>3</sub>, concentrations were around 307,000, 40,400, and 16,800, respectively [10].

As air pollution is strongly dependent on meteorological conditions [11,12], it is sensitive to climate change. According to the Sixth Assessment Report of the Intergovernmental Panel on Climate Change (IPCC) [13], it is expected that climate change will have complex effects on chemistry, transport, and the deposition of local air pollutants. IPCC also refers to urban areas as the ones that must respond to climate change risks [13,14], mostly due to the complex interactions between social, economic, and environmental stressors [15–17]. Indeed, climate change impacts in urban areas have recently become an important and urgent research topic. [18]. The full understanding of the links between climate change and air pollution in urban areas, and how they affect human health, are nowadays research challenges. Moreover, future emission scenarios should be considered due to their higher impact on air quality patterns, in line with the European Green Deal and the EU Clean Air Programme.

In the light of the above, the main aim of this work is to assess air pollution effects on human health at urban scale in the future, considering a given climate change scenario, through the application of a numerical modelling system, and using the Aveiro Region, in central Portugal, as a case study. This work will focus on the medium-term future (around 2050), following the Portuguese Roadmap for Carbon Neutrality in 2050 [19], under which Portugal has committed to prevent the increase of the global average temperature to well below 2 °C above pre-industrial levels, and to make efforts to limit the increase to 1.5 °C, in line with the Paris Agreement.

The Aveiro Region is located in the central part of Portugal, close to the Atlantic Ocean, with an area of 1693 km<sup>2</sup> and around 370,000 inhabitants. The Aveiro Region includes 11 municipalities, which are distinguished by their geography, economy, activity sectors, and population density [17,20]. The major economic sector of the region is the manufacturing industry, accounting for 50% of the region's income [21], followed by tourism, and services [20]. The most industrialized municipalities are typically located along the coast, closer to one of the most important seaports in Portugal. Rural municipalities, where agriculture plays an important role, are mainly situated in the inland parts of the region [22]. According to the Köppen climate classification [23], the Aveiro Region is classified as a warm-summer Mediterranean climate (Csb). Despite the climate and the open landscape characteristic of many municipalities in the Aveiro Region, which favour pollutants dispersion, PM and NO<sub>2</sub> exceedances occur occasionally in some areas of the region [17,20].

This work, easily applicable to other case studies, will fulfil the need for further studies that assess the future climate effects on air quality, with a high-resolution level, to support the identification of early climate and air pollution adaptation strategies. Additionally, several scientific communities, policymakers, and citizens, may benefit from the advances in the coordination between climate change, air quality, and health impact assessments for urban areas.

## 2. Data and Methods

This section presents the data and methodology used in this work, which can be divided in two parts, namely: (i) the WRF-CAMx modelling framework applied to assess the medium-term future climate and its impacts on air quality over the Aveiro Region (Section 2.1); and (ii) the health impact assessment (Section 2.2), based on WHO recommendations and considering the CAMx outputs.

### 2.1. Climate and Air Quality Modelling

To assess the future climate and air quality patterns in the study area, the WRF—Weather Research and Forecasting Model [24] together with the CAMx—Comprehensive Air Quality Model with Extensions [25] modelling framework was applied. These models

have been widely used to assess air pollution in different case studies worldwide, and more specifically in Portugal, with reliable and realistic results [12,17,26,27].

Three nested domains with increasing resolution at a downscaling ratio of five were used, with the outermost domain of 30 km horizontal resolution centred over the Iberian Peninsula, and the innermost domain of 1.2 km horizontal resolution, with  $75 \times 75$  horizontal grid cells, focusing on the Aveiro Region (Figure 1).

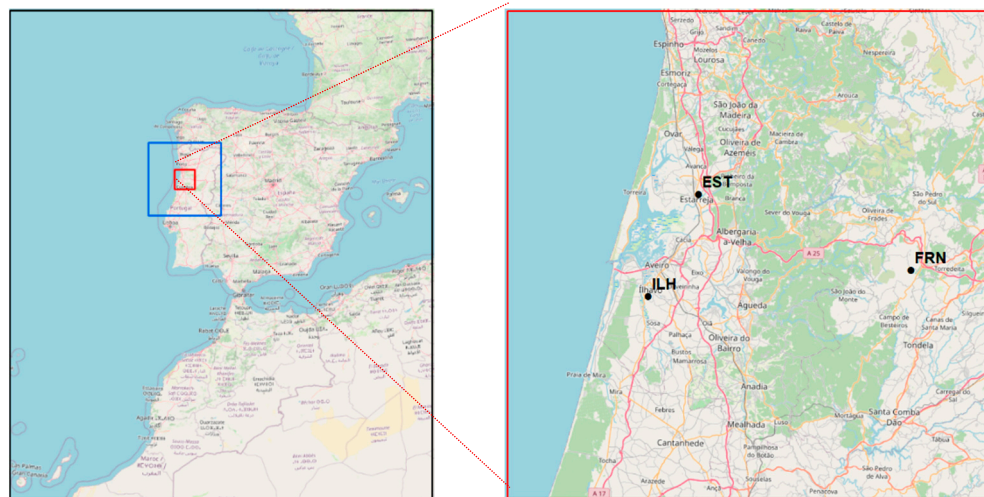


**Figure 1.** WRF-CAMx modelling system domains with 30 (D1—within the black rectangle), 6 (D2—within the blue square) and 1.2 (D3—within the red square) km resolution; and the location of the air quality monitoring stations (black points; EST: Estarreja—industrial background; ILH: Ílhavo—suburban background; and FRN: Fornelo do Monte—rural background).

The WRF model was forced by the Max Planck Institute for Meteorology Earth System Model version 1.2 (MPI-ESM1.2-HR) [28], with  $0.938^\circ$  horizontal resolution and 95 vertical levels. Other works [29,30] show that MPI-ESM is considered one of the best global models to predict the climate in Europe. Previous studies [30–32] also evaluated the use of MPI-ESM data as WRF forcing, thus ensuring the confidence in this model configuration for climate studies. The WRF physical configuration, selected based on previous studies [12,27,30,33,34], was as follows: microphysics—WRF Single-Moment 6-class scheme [35]; longwave and shortwave radiation—RRTMG [36]; surface layer—MM5 [37]; land surface—Noah [38]; planetary boundary layer—YSU [39]; cumulus—Grell-Freitas [40]; and sea surface temperature 6-hourly update. To keep the WRF downscaling consistent with the large-scale atmospheric dynamics of the forcing data, spectral nudging was used in the outermost domain for atmospheric waves larger than 1000 km in latitude and longitude.

The modelling system was applied for two years, one statistically representative of the recent past (2014), considered as a baseline, and the other statistically representative of the medium-term future climate (2055). As one of the objectives of this work is to focus on urban areas with a high-resolution level, the selection of representative years was a compromise to guarantee WRF-CAMx outputs with high spatial resolutions, avoiding excessively high computational efforts. Based on previous studies methodologies [12,34,41], the selection of the representative years was supported by a climatological analysis of every year of the periods 1995–2014 (for the recent past) and 2046–2065 (for the medium-term future), provided by coarser simulations, and compared with the average of each period, to find the year with the lowest climate anomaly. This analysis was performed for temperature, precipitation, wind direction, and solar radiation, as they are considered by the scientific community as fundamental for describing the climate [13] and are particularly important in air pollutants transport and deposition [42–45]. For the medium-term future climate, the new SSP2-4.5 (Shared Socio-Economic Pathway) scenario [46] was applied. As stated by Riahi et al. [47], SSP2-4.5 is part of the “middle of the road” socio-economic pathway, considering medium challenges for both climate change adaptation and mitigation and

a “medium pollution control” scenario, with a nominal  $4.5 \text{ W}\cdot\text{m}^{-2}$  radiative forcing level by 2100.

The CAMx initial and boundary (every 6 h) conditions for the outermost domain were provided by the Community Atmosphere Model with Chemistry (CAM-Chem [48]) global chemical model, with  $0.9^\circ \times 1.25^\circ$  spatial resolution. For the recent past climate, anthropogenic emissions were taken from the EMEP (European Monitoring and Evaluation Programme) emission inventory [49] and were spatially disaggregated according to the methodology described in Ferreira et al. [26] and speciated into the Carbon Bond 6 (CB6) chemical mechanism species considered in the CAMx simulation [50]. For the medium-term future climate, emissions were estimated by adapting the methodology defined by Sá et al. [51] and considering the emission projections from the Portuguese roadmap for carbon neutrality [19], in line with the SSP2-4.5 scenario considered in the WRF simulation. According to this methodology, medium-term future climate emissions, when compared to the recent past, show an average emission reduction of approximately 33% for PM10, 38% for PM2.5, 68% for NO<sub>x</sub>, 27% for NMVOC, 70% for CO, 15% for NH<sub>3</sub> and 35% for SO<sub>x</sub>. Note that these are average emission reductions for all source activities despite the emission projections foreseeing an increase for some activity sectors (e.g., NMVOC and PM10 in industrial combustion and processes sector, CO and NMVOC in agriculture, see Figure A1 of Appendix A).

## 2.2. Health Impacts Assessment

The effects of PM2.5, NO<sub>2</sub>, and O<sub>3</sub> long-term exposure on mortality have been reported in several epidemiological and toxicological studies [52]. Several studies [53–55] indicate that the exposure to PM2.5 is associated with damaged lung function, systemic inflammation and alteration of the electrical processes of the heart, as well as a causal association with cardiovascular and cardiorespiratory mortality. The associations of long-term NO<sub>2</sub> with respiratory and cardiovascular mortality, with effects on natural and cause-specific mortality, are similar to those estimated for PM2.5, according to several cohort studies [52,56–58]. Regarding O<sub>3</sub> long-term exposure, several cohort analysis suggested an effect on respiratory or cardiorespiratory mortality, especially in people with potential predisposing conditions [56,59,60]. For these pollutants, following the approach usually applied in the EEA (European Environment Agency) annual health assessments, described in Soares et al. [61], mortality health outcomes were analysed since it is the most serious health impact and the one with the most robust scientific evidence [62]. For O<sub>3</sub>, mortality due to respiratory diseases was considered, while for PM2.5 and NO<sub>2</sub>, all-cause (natural) mortality was considered, both at ages above 30 years. The health outputs were traduced in the number of premature deaths, for the population affected by air pollution living within the study area. According to the WHO [63], the health impact assessment can be performed in three major steps, namely: (i) population exposure assessment; (ii) health risk estimation; and (iii) uncertainty calculation. Figure 2 shows the health impact assessment scheme, with an example for PM2.5, long-term exposure, all-cause (natural) mortality, using WHO 2013 methodology and hypothetical concentration and population values.

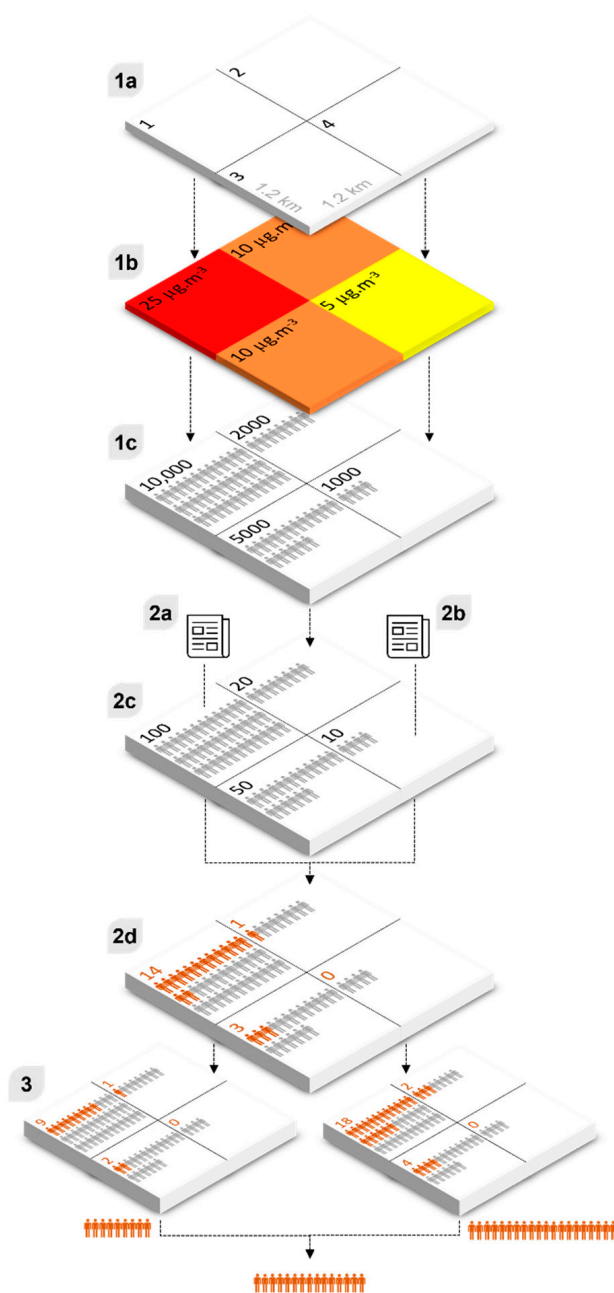


**Figure 2.** Health impact assessment scheme. Example for PM<sub>2.5</sub>, long-term exposure, all-cause (natural) mortality, using WHO 2013 methodology (adapted from [62]).

The main objective of the first step, the population exposure assessment, is to cross gridded pollutant concentration maps with gridded population data, at the same spatial resolution, resulting in a map with the population exposed, by grid cell, to the selected pollutant. For that, in the present work, the following data were used:

- CAMx surface concentrations results for PM<sub>2.5</sub>, NO<sub>2</sub>, and O<sub>3</sub>, by grid cell, for each period analysed (steps 1a and 1b in Figure 2 scheme);
- Most recent population data stratified by age and sex, from Census 2021, by the Portuguese national institute for statistics (INE) [64], for the recent past, and INE projection for 2050 [65] for the future, spatially disaggregated according to the CAMx grid (step 1c in Figure 2 scheme).

#### Population exposure assessment:

**(1a) Grid:** the area for which the health risk assessment will be calculated consists of a 4 cells grid with 1.2 × 1.2 km<sup>2</sup> horizontal resolution.

**(1b) Concentration Map:** the air quality modelling results, for cells 1 to 4, show PM<sub>2.5</sub> annual concentrations that vary between 5 and 15 µg·m<sup>-3</sup>, for the year under analysis.

**(1c) Population/Exposure:** the population is distributed across the grid and the exposure is calculated. For example, in cell 1, 10,000 inhabitants are exposed to 15 µg·m<sup>-3</sup> of PM<sub>2.5</sub>.

#### Health risk estimation:

**(2a) Baseline Concentration:** the baseline concentration for PM<sub>2.5</sub> is 0 µg·m<sup>-3</sup>, meaning that, for instance, for grid 1 the effect of the whole range of 25 µg·m<sup>-3</sup> of PM<sub>2.5</sub> will be estimated.

**(2b) Relative Risk:** in the case of PM<sub>2.5</sub>, the concentration-response function used for total (all-cause) mortality in people above 30 years of age implies a relative risk of 1062 per 10 µg·m<sup>-3</sup>. Thus, assuming linearity, an increase of 10 µg·m<sup>-3</sup> of PM<sub>2.5</sub> is associated with a 6.2% increase in total mortality in the total population considered.

**(2c) Mortality:** the total mortality (incidence base) in the country for the year under analysis and the population over 30 years of age is 10 deaths per 1000 inhabitants, so the number of deaths per grid is as shown.

**(2d) Premature Deaths:** the number of deaths attributed to exposure to PM<sub>2.5</sub> in each cell is obtained from:

$$\text{Relative Risk (RR)} = \exp(\beta * \text{concentration} - \text{baseline concentration}) = \exp(0.00602 * \text{concentration} - 0)$$

$$\text{For cell 1: } 1.162281$$

$$\text{Population Attributable Fraction (PAF)} = (RR - 1) / RR$$

$$\text{For cell 1: } 0.139623$$

$$\text{Premature Deaths (PD)} = \text{PAF} * \text{mortality} * \text{population}$$

$$\text{For cell 1: } 13.96 \approx 14$$

#### Uncertainty calculation:

**(3) Uncertainty:** the uncertainty range is calculated using the lower (1.040) and upper (1.083) limits of the relative risk of PM<sub>2.5</sub>, instead of 1.062.

**The total mortality is then expressed as 18 premature deaths, with a 95% confidence interval between 12 and 24.**

In the second step, health risk estimation, relative risk data from epidemiological studies and incidence mortality statistics are used, together with the population exposed from step 1, to assess the number of premature deaths, by grid cell, as shown in steps 2a to 2d in Figure 2 scheme. To apply it to the current case study, the following input data were used:

- Portuguese annual total number of deaths broken down by age, cohort and sex, from the European mortality database [48] (step 2c in Figure 2 scheme);
- Baseline concentration ( $C_0$ ) and concentration-response functions (CRF) were used for the estimation of the relative risk (RR) (2a and 2b from Figure 2 scheme) as follows:

$$RR = e^{\beta \cdot (C_i - C_0)}$$

where  $C_i$  is the concentration level the population is exposed to in grid cell  $i$  and  $\beta$  is the coefficient of the CRF. Assuming an exponential behaviour,  $\beta$  can be estimated based on the CRF:

$$CRF/UC = e^{\beta \cdot UC}$$

where CRF applied are described in Table 1 and  $UC = 10 \mu\text{g}\cdot\text{m}^{-3}$ .

For that, due to the recent update of the WHO air quality guidelines, two different methodologies were used: (i) the so-called WHO 2013, according to the recommendations of HRAPIE [66] and REVIHAAP [52] projects, considering CRF from Jerrett et al. [67] for  $\text{O}_3$  and from Hoek et al. [68] for  $\text{PM}_{2.5}$  and  $\text{NO}_2$ ; and (ii) the so called WHO 2021, according to the recommendations of new WHO air quality guidelines [6], considering CRF from Chen and Hoek [69] for  $\text{PM}_{2.5}$  and Huangfu and Atkinson [70] for  $\text{O}_3$  and  $\text{NO}_2$ . Table 1 presents detailed information on the CRF used, as well as a source of mortality data and  $C_0$ . From Table 1, major differences between the WHO 2013 and the WHO 2021 CRF methodologies can be found for mortality health outcomes associated with  $\text{PM}_{2.5}$  and  $\text{NO}_2$  long-term exposure. For  $\text{PM}_{2.5}$ , WHO 2021 considers a higher relative risk than WHO 2013. According to the WHO 2021 methodology, an increase in  $10 \mu\text{g}\cdot\text{m}^{-3}$  of  $\text{PM}_{2.5}$  is associated with an 8% increase in total mortality [68], while in WHO 2013 the increase in total mortality was only 6.2% [69]. However, WHO 2021 assumes a  $\text{PM}_{2.5}$  baseline concentration of  $5 \mu\text{g}\cdot\text{m}^{-3}$ , below which no health effects are expected, while WHO 2013 assumes expected health effects no matter the magnitude of  $\text{PM}_{2.5}$  concentrations. For  $\text{NO}_2$  the opposite happens, with a decrease in the relative risk from 5.5% [68] in WHO 2013 to 2% [70] in WHO 2021, and the assumption that lower concentrations (above  $10 \mu\text{g}\cdot\text{m}^{-3}$ , rather than above  $20 \mu\text{g}\cdot\text{m}^{-3}$  in WHO 2013) may have health impacts. The new baseline concentrations were determined by the WHO [6], using the average of the five lowest 5th percentile levels measured in five selected studies for  $\text{PM}_{2.5}$  [71–75] and  $\text{NO}_2$  [76–80].

**Table 1.** CRF used according to the WHO 2013 [52,66] and WHO 2021 [6] recommendations.

Pollutant	RR per $10 \mu\text{g}\cdot\text{m}^{-3}$ (95% CI)		Baseline Concentration ( $C_0$ )		Source of Mortality Data	Health Outcome
	WHO 2013	WHO 2021	WHO 2013	WHO 2021		
PM <sub>2.5</sub> , annual mean	1.062 (1.040; 1.083), in [68]	1.08 (1.06; 1.09), in [69]	>0 $\mu\text{g}\cdot\text{m}^{-3}$	>5 $\mu\text{g}\cdot\text{m}^{-3}$	European mortality database in [81], ICD-10: A-R	Mortality, all-cause (natural), age 30+ years
NO <sub>2</sub> , annual mean	1.055 (1.031; 1.080), in [68]	1.02 (1.01; 1.04), in [70]	>20 $\mu\text{g}\cdot\text{m}^{-3}$	>10 $\mu\text{g}\cdot\text{m}^{-3}$		
O <sub>3</sub> , SOMO35 <sup>1</sup>	1.014 (1.005; 1.024), in [67]	1.01 (1.00; 1.02), in [70]	>70 $\mu\text{g}\cdot\text{m}^{-3}$	>70 $\mu\text{g}\cdot\text{m}^{-3}$	European mortality database in [81], ICD-10: J00-J99	Mortality, respiratory diseases, age 30+ years

<sup>1</sup> Summer months (April–September), average of daily maximum 8-h mean over 35 ppb.

The contribution of a risk factor to a premature death can be estimated by means of population attributable fraction (*PAF*), that can be calculated from the *RR*, for every grid cell *i*, as follows:

$$PAF = (RR - 1) / RR$$

Thus, the premature deaths (*PD*) can be estimated from *PAF*, assuming the baseline incidence as the crude death rates by age *a* and sex *s* (*CDR<sub>a,s</sub>*) and the population at grid cell *i* (*pop<sub>i</sub>*), as follows:

$$PD = \sum_{a,s} CDR_{a,s} \cdot pop_i \cdot PAF$$

In step three, the uncertainty associated with the health risk estimation is calculated. Most of the uncertainty is related to the *CRF* used, since it derives from the assumptions made in epidemiological studies that take into account other confounding factors that can also have an impact on mortality (e.g., smoking, diet, lifestyle) [63]. Thus, following the EEA approach [61], the uncertainty is calculated using a 95% confidence interval, indicating that there is a 95% probability that the true value lies in the range defined by the interval. Finally, after the population exposure assessment, the health risk estimation and the uncertainty calculation, the total mortality due to PM<sub>2.5</sub>, NO<sub>2</sub> and O<sub>3</sub> long-term exposure was assessed.

Additionally, following the EEA approach [61], the years of life lost (*YLL*) indicator was also estimated as a mortality-related health outcome. *YLL* is defined as the years of potential life loss due to premature death. It is an estimate of the average number of years that a person would have lived if the person would not have died prematurely. *YLL* considers the age at which death occurs and is greater for deaths at a younger age and lower for deaths at an older age [82]. It gives, therefore, more nuanced information than the number of *PD* alone. *YLL* is determined by relating *PD* with life expectancy (*LE*) by sex *s* and age *a*, for every grid cell *i*:

$$YLL = \sum_{a,s} LE_{a,s} \cdot PD$$

where *LE<sub>a,s</sub>* is the average time a person is expected to live, based on the year of their birth, their current age and sex (available in Census 2021 [64]).

### 3. Results and Discussion

This section presents the analysis and discussion of the obtained results for climate and air quality (Section 3.1), and for the health impact assessment (Section 3.2), for the reference and medium-term future.

#### 3.1. Climate and Air Quality Modelling

For both climate and air quality assessment, results obtained for the medium-term future climate were compared with the results for the recent past. The comparison was made for the following periods: (i) annual; (ii) spring (March to May); (iii) summer (June to August); (iv) autumn (September to November); and (v) winter (December to February).

For the climate change assessment, mean temperature and total precipitation were analysed. Figure 3 shows the annual average of mean temperature and total precipitation, for the medium-term future climate, recent past climate, and the difference between them. Seasonal results can be found in Appendix A, in Figures A2 and A3.

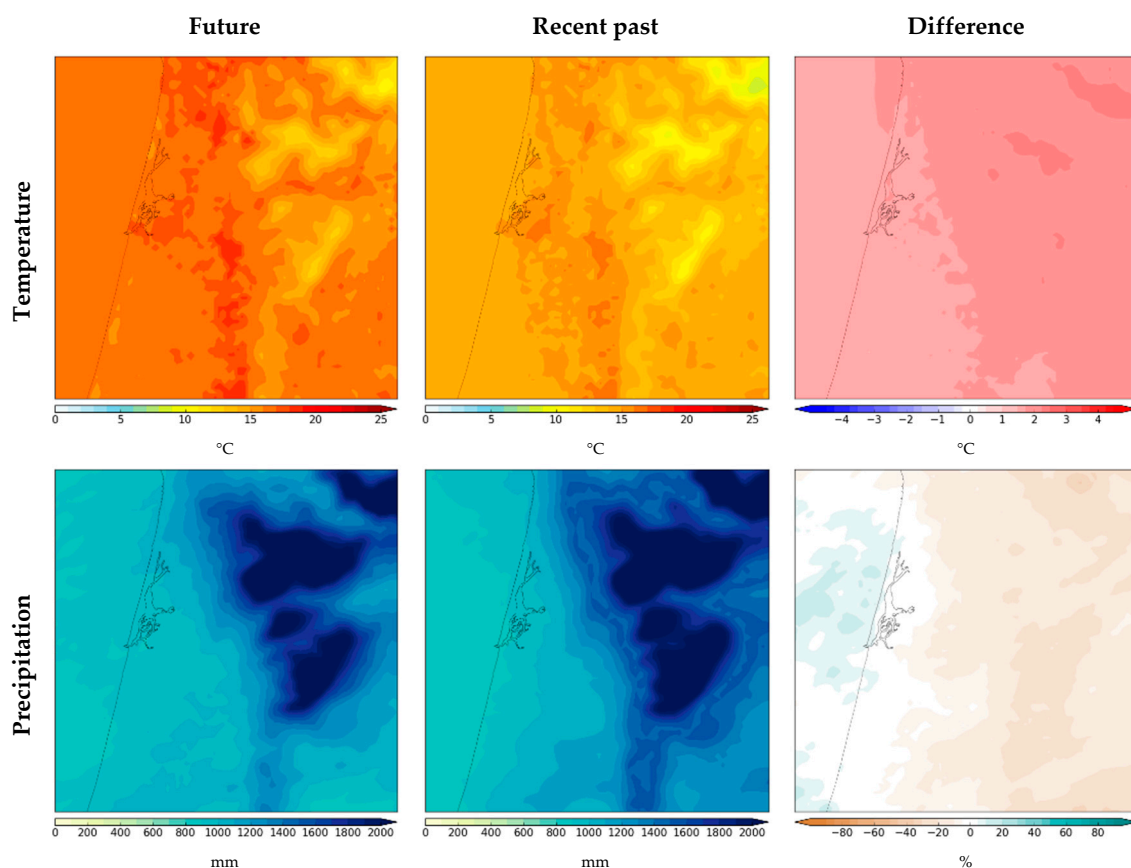


**Figure 3.** Annual mean temperature and total precipitation, for the medium-term future climate (2055), recent past climate (2014) and the difference between them (2055–2014).

The differences between the medium-term future climate and the recent past climate for the annual mean temperature, show an increase in future temperature between 1 and 2 °C, with lower differences estimated closer to the coastline and in the lower altitude areas. For the annual total precipitation, a decrease of up to 40% is expected in some areas of the region. Over the coastline, no differences are projected in total precipitation and an increase, between 10 and 20%, is predicted over some parts of the Atlantic Ocean. Notwithstanding, in agreement with what has been shown in other studies [13], a trend toward reduced precipitation in the medium-term future is clear. This precipitation trend, together with the higher temperatures projected, will lead to drier conditions, as has been already observed in southern Europe countries [83]. Regarding the seasonal analysis, the results show different variations. The highest temperature differences are projected for the summer, where the mean temperature can increase up to 4 °C, and the lowest differences are projected for autumn, with some parts of the study region for which differences are not expected. Moreover, for none of the seasons, is a temperature decrease expected in the future. Differences in precipitation also exhibit several variations across the seasons. For summer and autumn, a precipitation reduction of around 80% and 45%, respectively, is expected in almost the entire study region. However, in winter and spring, the precipitation decrease projected for the medium-term future is only foreseen for the inland regions of the domain, with an expected increase over the Atlantic Ocean and coastal areas. These results are in line with previous studies [12,27,30,33,84], which also project higher temperatures and lower total precipitation, even though they are applied to other case studies, using different climate change scenarios, and/or considering distinct future periods. Greater warming over land will change key features of water cycle, affecting the precipitation variability [13]. According to other studies [13,85], it is expected a precipitation increase over high latitudes and oceans, and a decrease over large parts of the subtropics in response

to greenhouse gas-induced warming. Thus, coastal areas will be the zones with the smaller changes, as it is where the climate change signals change the sign [84]. The projected decrease in precipitation over land, amplified by the high evapotranspiration related to strong warming, could also lead to more frequent and intense periods of drought [33,83,85].

These future climate patterns will have complex effects on chemical reactions, transport, dispersion, and the deposition of air pollutants [43]. Temperature affects the chemical reaction rates as well as the dispersion and deposition of chemical compounds [44,45]. The precipitation washout also plays an important role in removing pollutants from the atmosphere, by wet deposition [86,87]. Figure 4 shows the annual average concentration of  $\text{NO}_2$ ,  $\text{PM}_{10}$ , and  $\text{PM}_{2.5}$ , and the annual average concentration of the maximum daily 8 h mean  $\text{O}_3$ , for the medium-term future climate, the annual average, recent past climate, and the difference between them. Seasonal results can be found in Appendix A, in Figures A4–A7.

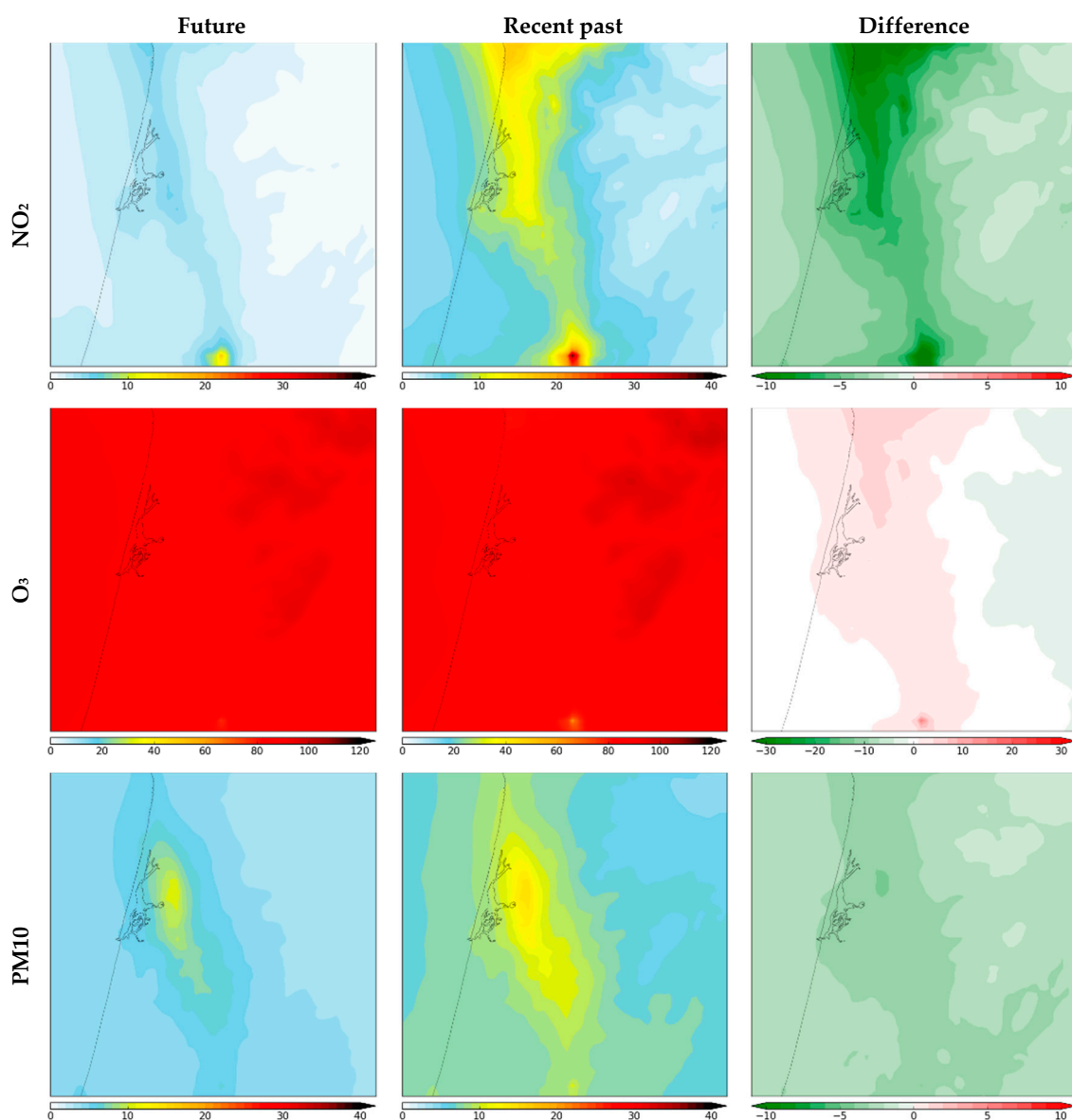
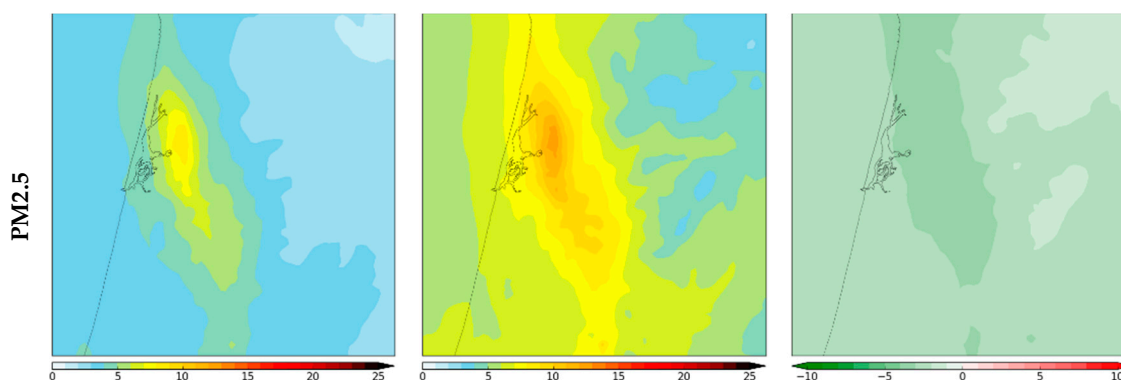


Figure 4. Cont.



**Figure 4.** Annual average concentration of NO<sub>2</sub>, PM10, and PM2.5, and the annual average concentration of the maximum daily 8 h mean O<sub>3</sub>, in  $\mu\text{g}\cdot\text{m}^{-3}$ , for the medium-term future climate (2055), recent past climate (2014) and the difference between them (2055–2014). For future and recent past maps, the maximum value of the colour scale represents the EU limit value.

For both periods analysed, medium-term future and recent past climate, all pollutants show similar spatial patterns, but with different magnitudes of the concentrations. The differences between the medium-term future climate and the recent past climate, result in a decrease in the annual average concentration of NO<sub>2</sub>, PM10, and PM2.5 up to 10, 4, and 3  $\mu\text{g}\cdot\text{m}^{-3}$ , respectively. For the medium-term future climate, the differences in the annual average concentration of the maximum daily 8 h mean O<sub>3</sub> show decreases (up to 4  $\mu\text{g}\cdot\text{m}^{-3}$ ) and increases (up to 10  $\mu\text{g}\cdot\text{m}^{-3}$ ), depending on the area. When analysed seasonally, O<sub>3</sub> shows variations along the seasons, while the remaining pollutants maintain a similar behaviour to the annual one. For NO<sub>2</sub>, major differences are found in the same areas where higher concentration values are obtained for the recent past, namely: (i) in the north of the domain, where part of the Porto metropolitan area (the second largest urban area in Portugal) is located, and that influences Aveiro Region air quality due to the pollutants transport by the north/northwest dominant winds; and (ii) in a small area in the south, the site of one of the major cement factories in Portugal. The 68% of NO<sub>x</sub> emission reduction projected for the future, mostly related to transportation, industry and energy sectors (see Figure A1 of Appendix A), will lead to this reduction in the NO<sub>2</sub> concentrations. In contrast, in the locations with higher NO<sub>2</sub> concentration reductions, an air quality deterioration due to O<sub>3</sub> pollution will be expected, due to the reduction of NO<sub>x</sub> values, but also due to the projected temperature increase, favouring photochemical phenomena. Concerning PM10 and PM2.5 results, higher concentrations were estimated over the most industrialized areas of the Aveiro Region, where major concentration reductions are also projected for the future. Although a decrease in total precipitation is expected in the Aveiro Region, which could lead to an increase in both PM10 and PM2.5 concentrations [86,87], this does not happen due to the reduction of the future PM emissions considered. These results are in line with previous studies applied for Portuguese case studies, e.g., [88–90], as well as for other countries/regions e.g., [91–93]. Similarly to what was verified in the current study, Sá et al. [90] recorded a decrease of the NO<sub>2</sub> (around 15%), and an increase of O<sub>3</sub> (up to 3%) annual mean concentrations in Portuguese coastal regions. Lacressonnière et al. [91] projected a decrease in PM10 and NO<sub>x</sub> annual mean concentration, around 2.1  $\mu\text{g}\cdot\text{m}^{-3}$  for both pollutants, and an increase, up to 21.6  $\mu\text{g}\cdot\text{m}^{-3}$ , for O<sub>3</sub>, for continental Europe in 2030.

For the medium-term future, the projected decrease in NO<sub>2</sub>, PM10, and PM2.5 annual concentrations will ensure that the limit values imposed by the European Union Air Quality Directive [5] will not be exceeded. For the same period, despite the projected increase in the maximum daily 8 h mean O<sub>3</sub> concentrations, they will also be below the defined target values for the protection of human health. However, if the new WHO air quality guidelines [6] are considered, the future annual concentration of PM2.5 and maximum daily 8 h mean O<sub>3</sub> will be above the recommended air quality guideline levels (5 and 60  $\mu\text{g}\cdot\text{m}^{-3}$ , respectively), in some areas of the Aveiro Region.

To give an insight into the accuracy of the presented results, the CAMx performance was evaluated through the application of performance statistics, based on the monitored NO<sub>2</sub>, O<sub>3</sub>, and PM10 concentrations during 2014, from the Air Quality e-Reporting database [94], for the three air quality monitoring stations identified in Figure 1. In general, the CAMx tends to underestimate NO<sub>2</sub> and PM10 concentrations, while O<sub>3</sub> concentrations tend to be overestimated. However, according to the FAIRMODE guidelines [95], the obtained results fulfil the modelling quality objective, defined as the minimum level of quality to be achieved by a model for policy use. For a detailed quantitative analysis of the CAMx performance, see Appendix A, Table A1.

### 3.2. Health Impact Assessment

Premature deaths, due to PM2.5, NO<sub>2</sub>, and O<sub>3</sub> long-term exposure, for the mid-term future climate, the recent past climate, and the difference between them, considering both the WHO 2013 and the WHO 2021 CRF methodologies, are shown in Table 2.

**Table 2.** Premature deaths and YLL, due to PM2.5, NO<sub>2</sub>, and O<sub>3</sub> long-term exposure, for the medium-term future climate (2055), recent past climate (2014) and the difference between them (2055–2014), considering both the WHO 2013 and the WHO 2021 CRF methodologies. Premature deaths and YLL considering the 95% confidence interval are shown in brackets. Note that negative values mean avoided premature deaths and YLL.

Pollutant	Health Outcome	WHO 2013			WHO 2021		
		Future	Recent Past	Difference	Future	Recent Past	Difference
PM2.5, annual mean	Premature deaths	3297 (1914; 4836)	6945 (3864; 9767)	−3648 (−1950; −4931)	93 (49; 109)	2234 (1579; 2546)	−2141 (−1530; −2437)
	YLL	34,029 (19,124; 50,281)	73,823 (40,185; 105,728)	−39,794 (−21,061; −55,446)	891 (472; 1044)	22,699 (15,706; 26,260)	−21,808 (−15,234; −25,216)
NO <sub>2</sub> , annual mean	Premature deaths	0 (0; 0)	13 (6; 21)	−13 (−6; −21)	0 (0; 0)	241 (83; 560)	−241 (−83; −560)
	YLL	0 (0; 0)	124 (58; 213)	−124 (−58; −213)	0 (0; 0)	2472 (794; 6113)	−2472 (−794; −6113)
O <sub>3</sub> , SOMO35	Premature deaths	0 (0; 0)	0 (0; 0)	0 (0; 0)	0 (0; 0)	0 (0; 0)	0 (0; 0)
	YLL	0 (0; 0)	0 (0; 0)	0 (0; 0)	0 (0; 0)	0 (0; 0)	0 (0; 0)

When considering the WHO 2013 CRF methodology, PM2.5 long-term exposure led to 3297 (95% CI: 1914 to 48,369) and 6945 (95% CI: 3864 to 9767) premature deaths in the medium-term future and recent past climate, respectively, representing around 53% of premature deaths avoided in the future. These premature deaths represent 73,823 (95% CI: 40,185 to 105,728) YLL in the recent past climate and 34,029 (95% CI: 19,124 to 50,281) in the medium-term future climate. For NO<sub>2</sub>, 13 premature deaths, with a 95% CI between 6 and 21, are estimated for the recent past climate, accounting for 124 YLL, with a 95% CI between 58 and 213. For the future no premature deaths and YLL are expected. If the WHO 2021 CRF methodology is considered, PM2.5 long-term exposure led to 93 (95% CI: 49 to 109) premature deaths and 891 (95% CI: 472 to 1044) YLL in the medium-term future, meaning around 96% of premature deaths and YLL avoided, when compared to the recent past values. For NO<sub>2</sub>, 241 premature deaths and 2472 YLL are estimated in the recent past climate, with a 95% CI between 83 and 560, and between 794 and 6113, respectively, and, as for the WHO 2013 CRF methodology, no premature deaths and YLL are expected for the future. For both CRF methodologies and periods considered, O<sub>3</sub> long-term exposure will not result in premature deaths and YLL. Regardless of the CRF methodology used, there will be a reduction in the number of premature deaths and the associated YLL, related to PM2.5 and NO<sub>2</sub> long-term exposure, due to the projected air quality improvement for the medium-term future. However, premature deaths and YLL will also continue to occur in the future, due to long-term exposure to PM2.5 pollution, even if in a smaller number. From Table 2 it can be also concluded that the use of different CRF

methodologies could substantially impact the estimated number of premature deaths and *YLL*. When considering the WHO 2021 methodology, the changes in the relative risk and baseline concentration used will impact the estimation of the health risk and, consequently the number of premature deaths and *YLL*. For PM<sub>2.5</sub>, although there is an increase in the relative risk, the reduction of the considered range concentrations from all to only above  $5 \mu\text{g}\cdot\text{m}^{-3}$ , associated with the baseline concentration used, led to a reduction in the number of premature deaths and the associated *YLL*. However, for NO<sub>2</sub>, the opposite is verified, with an increase in premature deaths, and consequently on *YLL*, mainly due to the change in the baseline concentration. Additionally, the confidence interval shows some changes, with a smaller range between the lower and upper values, due to the changes in the lower and upper relative risk considered.

To better understand where premature deaths are expected to occur, maps of mortality due to NO<sub>2</sub> and PM<sub>2.5</sub> long-term exposure were also produced and are presented in Figure 5. For the two periods and the *CRF* methodologies considered, O<sub>3</sub> mortality maps were not drawn as no premature deaths were obtained.

The projected premature deaths associated with NO<sub>2</sub> and PM<sub>2.5</sub> show similar spatial patterns for medium-term future climate and recent past climate, but with different magnitudes of values. According to Figure 5, premature deaths are mostly obtained near the coastline, where the population density is higher, with special relevance in the Porto metropolitan area, in the north of the domain, but also highly industrialized areas, such as the one in the Aveiro Region, where higher pollutant concentrations were previously obtained. Regarding the effects of the *CRF* methodology used in the spatial distribution of premature deaths, this is more evident for NO<sub>2</sub>. When using the WHO 2021 methodology, with the reduction of the baseline concentration value, the relevance of NO<sub>2</sub> concentrations in urban areas is highlighted, as shown in Figure 5, where premature deaths are foreseen in the Porto metropolitan area. The same is not true when the WHO 2013 methodology is used. As already analysed in Table 2, regardless of the *CRF* methodology used, in the medium-term future climate there will be a reduction in the number of premature deaths related to both NO<sub>2</sub> and PM<sub>2.5</sub> long-term exposure.

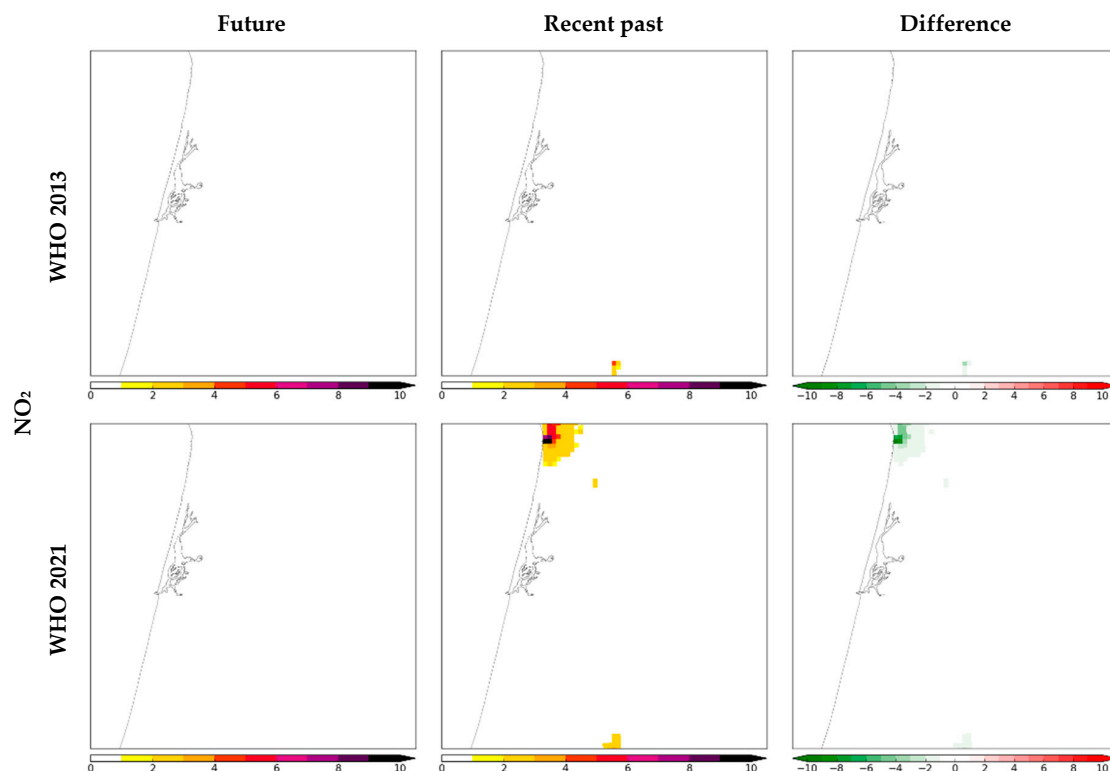
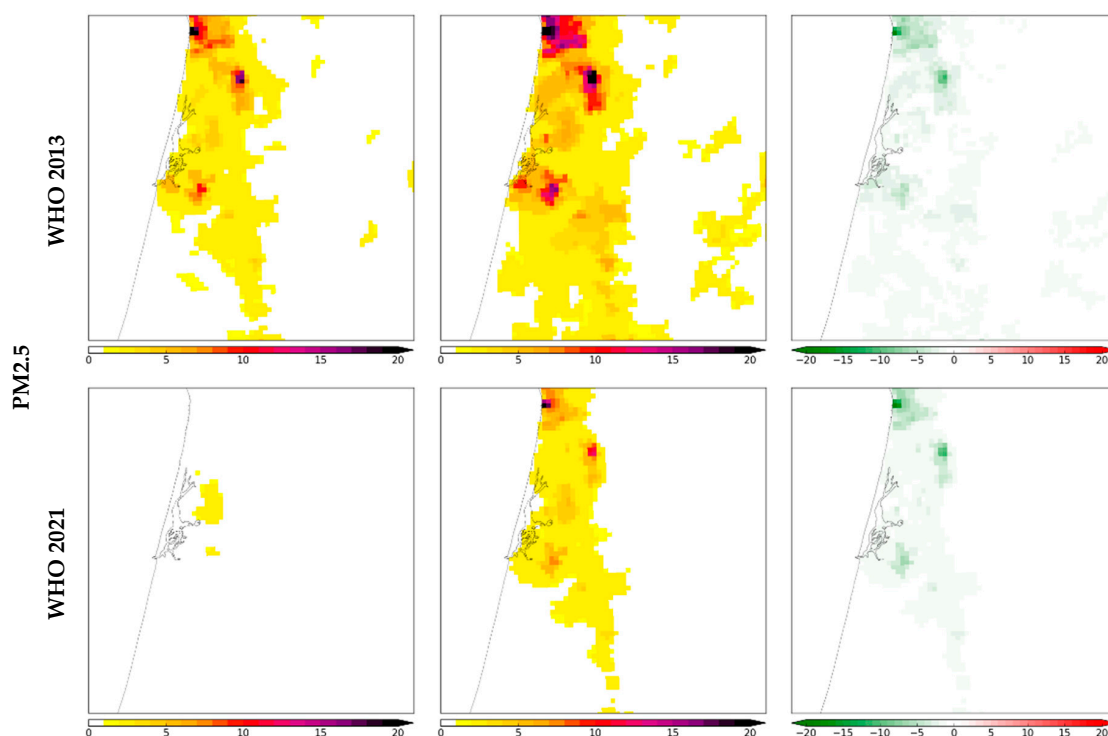


Figure 5. Cont.



**Figure 5.** Mortality due to  $\text{NO}_2$  and  $\text{PM}_{2.5}$  long-term exposure, expressed in number of premature deaths, for the medium-term future climate (2055), recent past climate (2014) and the difference between them (2055–2014), considering both the WHO 2013 and the WHO 2021 CRF methodologies. Note that negative values mean avoided premature deaths.

For the recent past climate, these results are in line with those obtained by EEA [96]. Although the reference and future years are different, as well as the climate change scenario and the applied case study, the studies from Silva et al. [97], Partanen et al. [98], and Likhvar et al. [99], also projected a decrease in the number of premature deaths due to air pollutants long-term exposure, in the future.

#### 4. Conclusions

In this work, the WRF-CAMx modelling system, followed by a health impact assessment, was applied to the Aveiro Region urban area, in Central Portugal. Climate change results for the medium-term future climate, when compared with the recent past climate, project higher mean temperature and lower total precipitation for the Aveiro Region. Despite these results, general improvements in air quality are foreseen, with no exceedances to the EU air quality limited values, mainly due to the reduction in future emissions imposed by European legislation. Nonetheless, some concerns regarding  $\text{PM}_{2.5}$  and  $\text{O}_3$  concentrations remain when the new WHO air quality recommendation levels are considered. Following the air quality trend, mortality due to pollutants' long-term exposure will also decrease, with only premature deaths related to  $\text{PM}_{2.5}$  pollution being expected, regardless of the CRF methodology used (WHO 2013 or WHO 2021).

Although this joint analysis of climate change, air quality, and health impacts give valuable information on these research fields, some limitations can be identified, and caution should be taken in using these results. As for all studies based on numerical modelling, uncertainties resulting from the modelling formulations and parameterizations, the input data (e.g., meteorology, emission inventories, population data), the CRF methodology, as well as the spatial resolution used, can affect the model results accuracy and also the reliability of the health impact assessment. Additionally, land use patterns will be influenced by climate change, and will impact emissions and, consequently, air quality, thus land use changes should be considered in future works.

Moreover, this study allowed to conclude that the use of different CRF methodologies in the health impact assessment could substantially impact the number of premature deaths. This evidences the magnitude of uncertainty related to the estimation of health impacts of air pollution and reinforces the need for an adequate awareness when communicating this type of scientific results to stakeholders and the general population.

Notwithstanding, the methodology applied in this work constitutes an added value in this research field, providing valuable information for policymakers and helping citizens increase awareness about climate change, air pollution, and human health impacts. Furthermore, both modelling and epidemiologist scientific communities may apply the developed methodology in other areas and benefit from advances in the harmonization between climate change, air quality, and health impact assessments for urban areas.

**Author Contributions:** Conceptualization and methodology, S.C. and J.F.; formal analysis, investigation, and writing—original draft preparation, S.C.; writing—review and editing, J.F., D.C., and M.L.; supervision, J.F. and M.L. All authors have read and agreed to the published version of the manuscript.

**Funding:** Thanks are due to the financial support to the PhD grant of S. Coelho (SFRH/BD/137999/2018), the contract grants of J. Ferreira (2020.00622.CEECIND) and D. Carvalho (2020.00563.CEECIND), and to CESAM (UIDP/50017/2020+ UIDB/50017/2020+ LA/P/0094/2020), to FCT/MCTES through national funds and the co-funding by the FEDER, within the PT2020 Partnership Agreement and Compete 2020.

**Institutional Review Board Statement:** Not applicable.

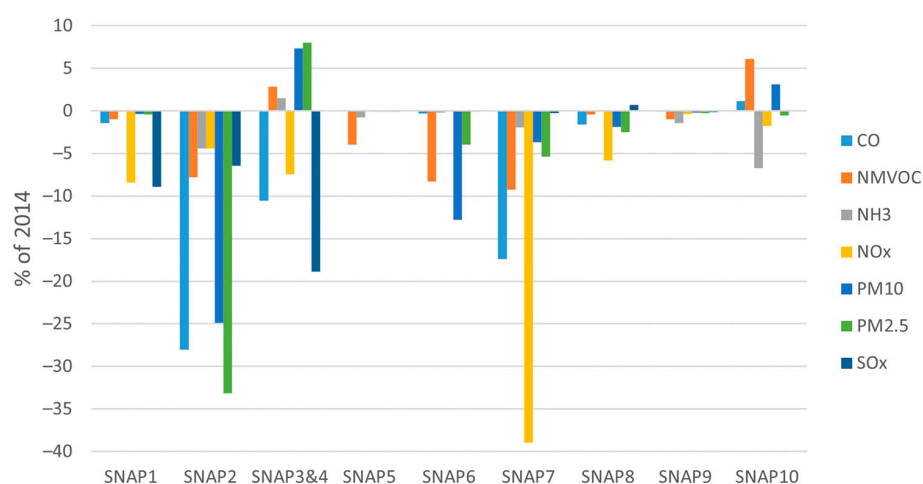
**Informed Consent Statement:** Not applicable.

**Data Availability Statement:** The relevant data underlying this study are fully available under the details provided in the references. For further questions, please contact the corresponding author.

**Conflicts of Interest:** The authors declare no conflict of interest.

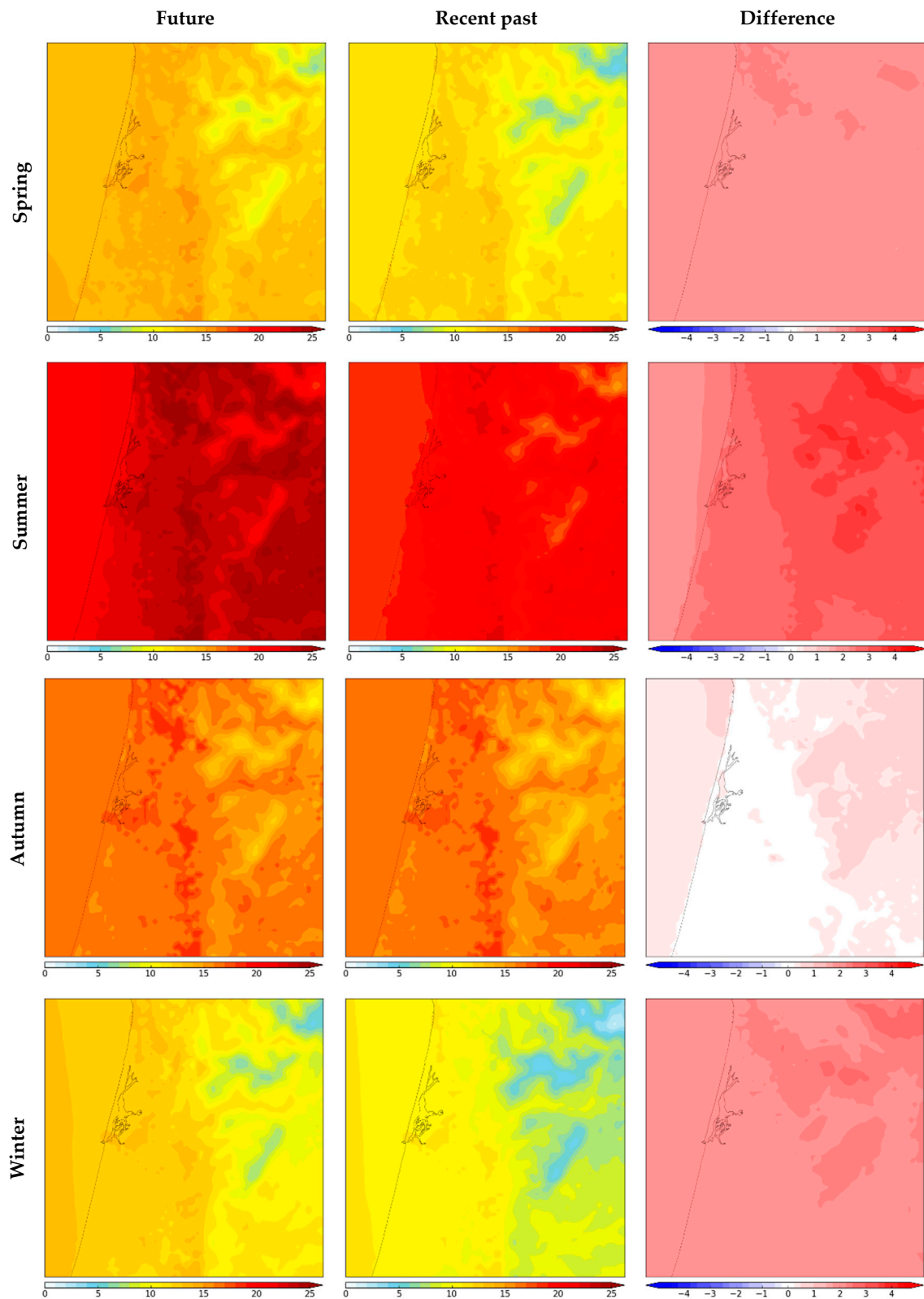
## Appendix A

Figure A1 shows the medium-term future emission projections from the Portuguese roadmap for carbon neutrality [19], expressed in % of the 2014 total emission, for CO, NMVOC, NH<sub>3</sub>, NO<sub>x</sub>, PM<sub>10</sub>, PM<sub>2.5</sub>, and SO<sub>2</sub>, by source activity.



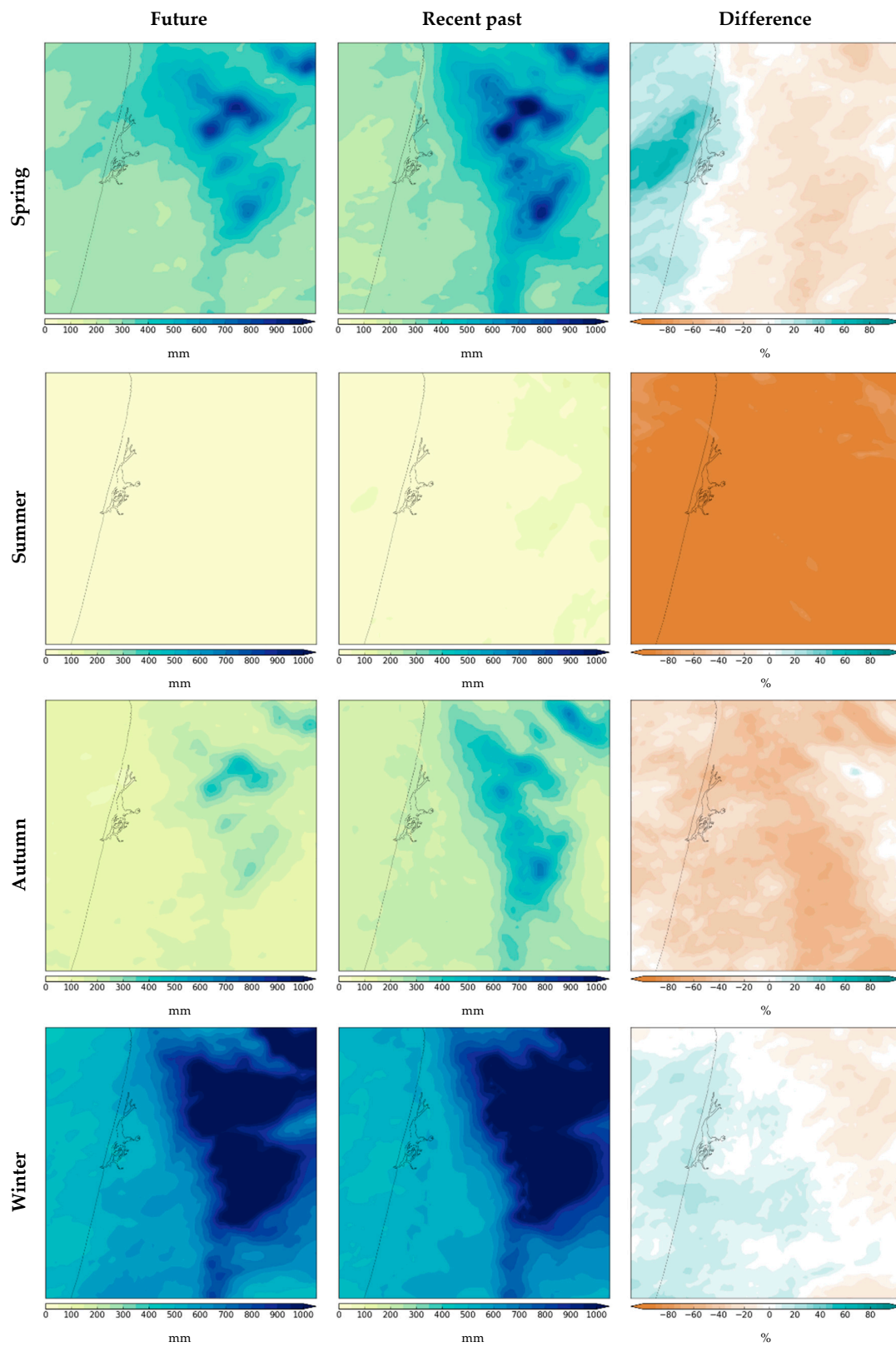
**Figure A1.** Medium-term future emission projections from the Portuguese roadmap for carbon neutrality [19], expressed in % of the 2014 total emission, for CO, NMVOC, NH<sub>3</sub>, NO<sub>x</sub>, PM<sub>10</sub>, PM<sub>2.5</sub>, and SO<sub>2</sub>, by source activity (SNAP1—energy industries; SNAP2—residential and commercial combustion; SNAP 3&4- industrial combustion and processes; SNAP5—extraction and distribution of fossil fuels; SNAP6—solvent use; SNAP7—road transport; SNAP8—non-road transport and other mobile sources; SNAP9—waste treatment; and SNAP10—agriculture).

Figure A2 shows the seasonal mean temperature, in  $^{\circ}\text{C}$ , for the medium-term future climate, recent past climate, and the difference between them.



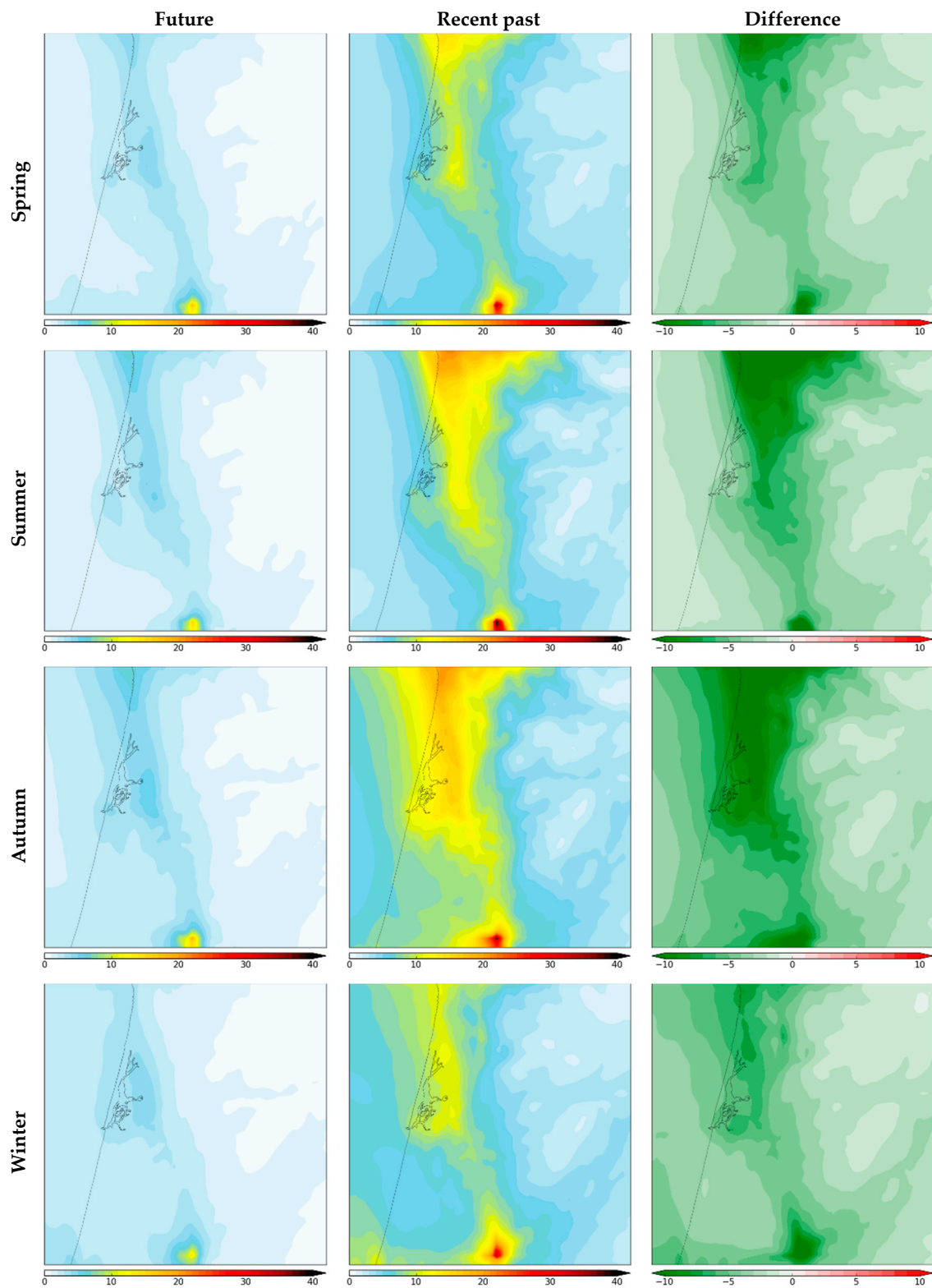
**Figure A2.** Seasonal average of mean temperature, in  $^{\circ}\text{C}$ , for the medium-term future climate (2055), recent past climate (2014), and the difference between them (2055–2014).

Figure A3 shows the seasonal total precipitation, for the medium-term future climate, recent past climate, and the difference between them.



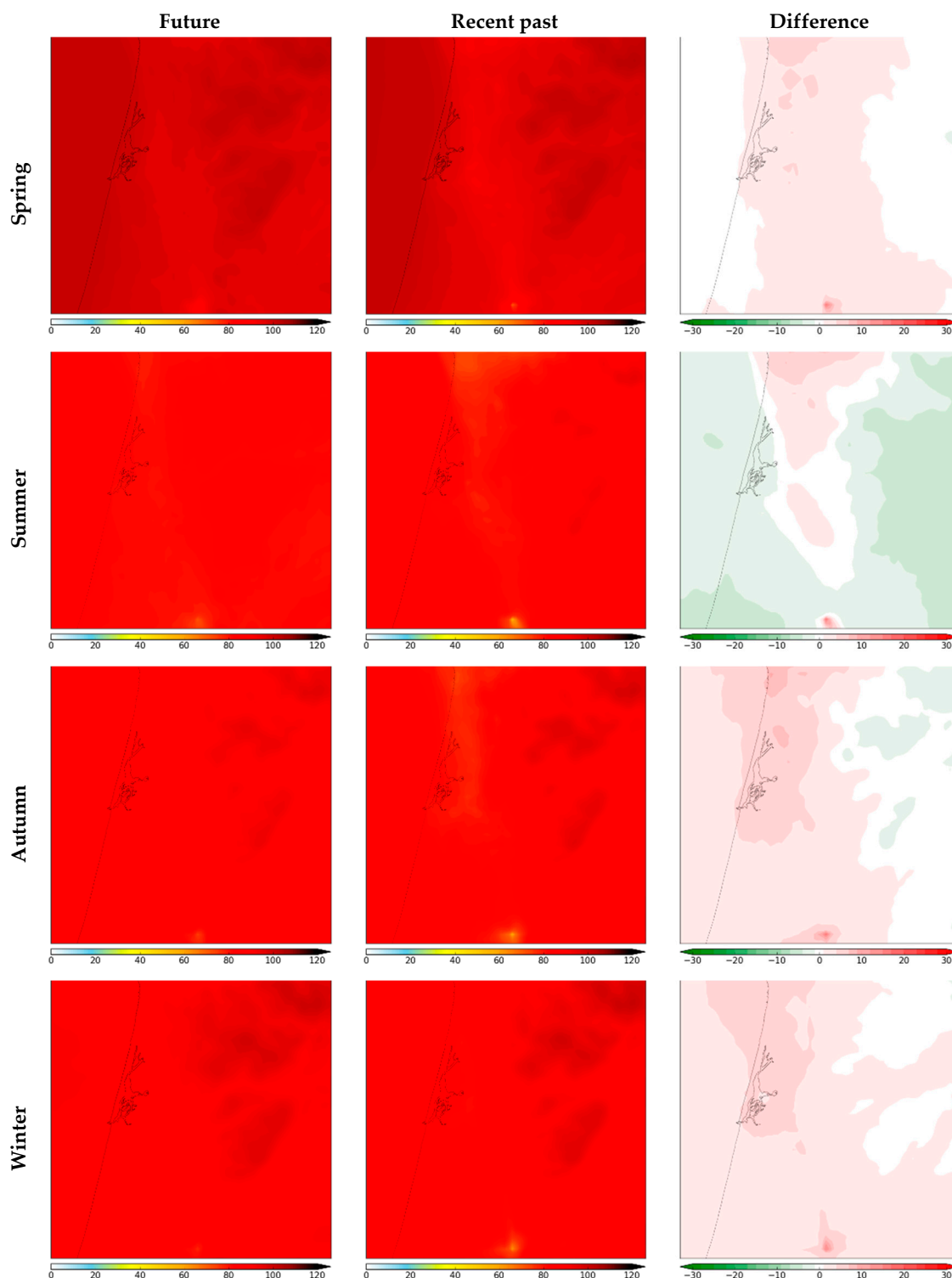
**Figure A3.** Seasonal total precipitation, for the medium-term future climate (2055), recent past climate (2014), in mm, and the difference between them (2055–2014), in %.

Figure A4 shows seasonal average concentrations of NO<sub>2</sub>, for the medium-term future climate, recent past climate, and the difference between them.



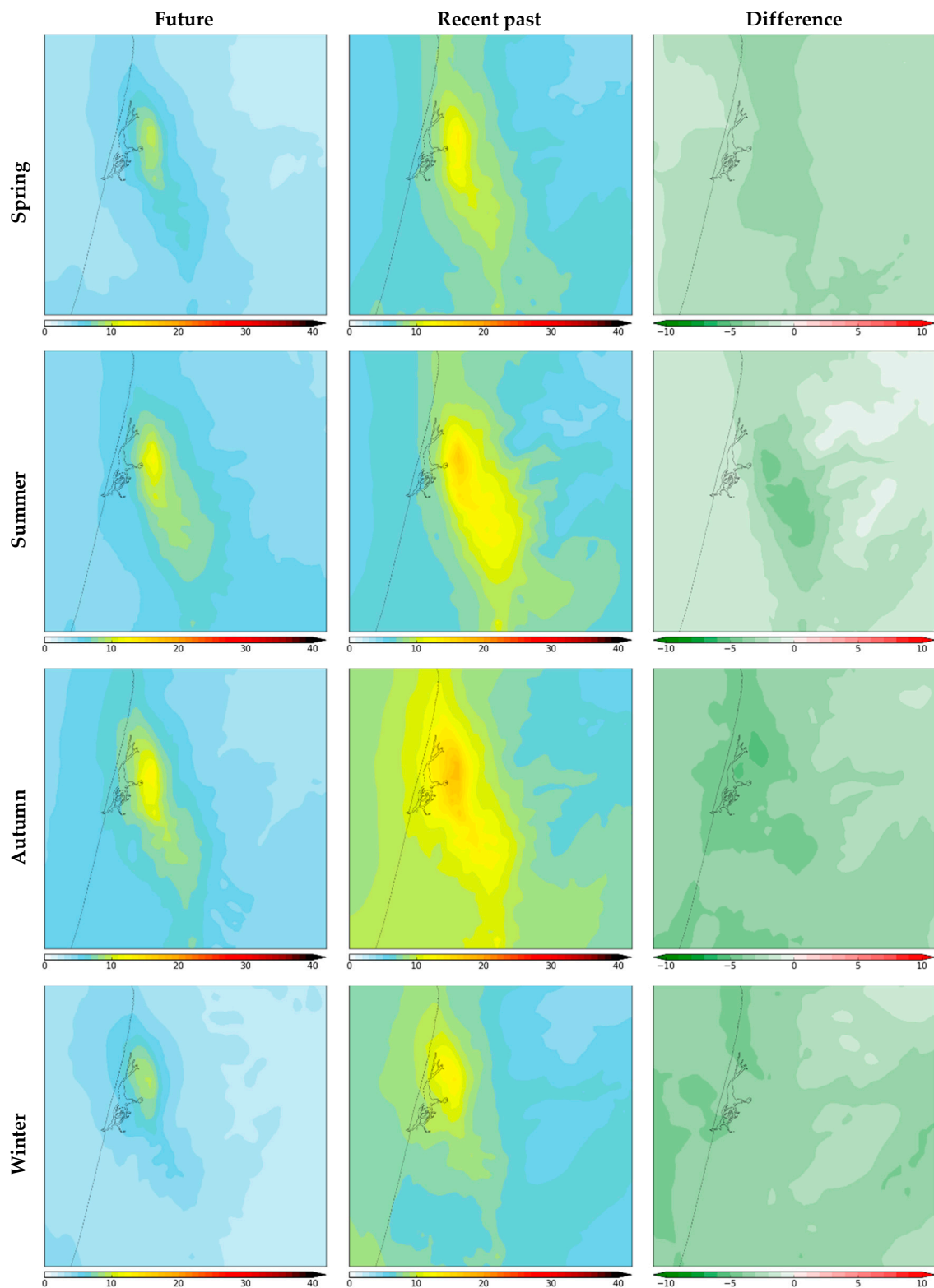
**Figure A4.** Seasonal average concentrations of NO<sub>2</sub>, in µg·m<sup>-3</sup>, for the medium-term future climate (2055), recent past climate (2014), and the difference between them (2055–2014). For future and recent past maps, the maximum value of the colour scale represents the EU limit value (40 µg·m<sup>-3</sup>).

Figure A5 shows seasonal average concentrations of the maximum daily 8 h mean  $O_3$ , for the medium-term future climate, recent past climate, and the difference between them.



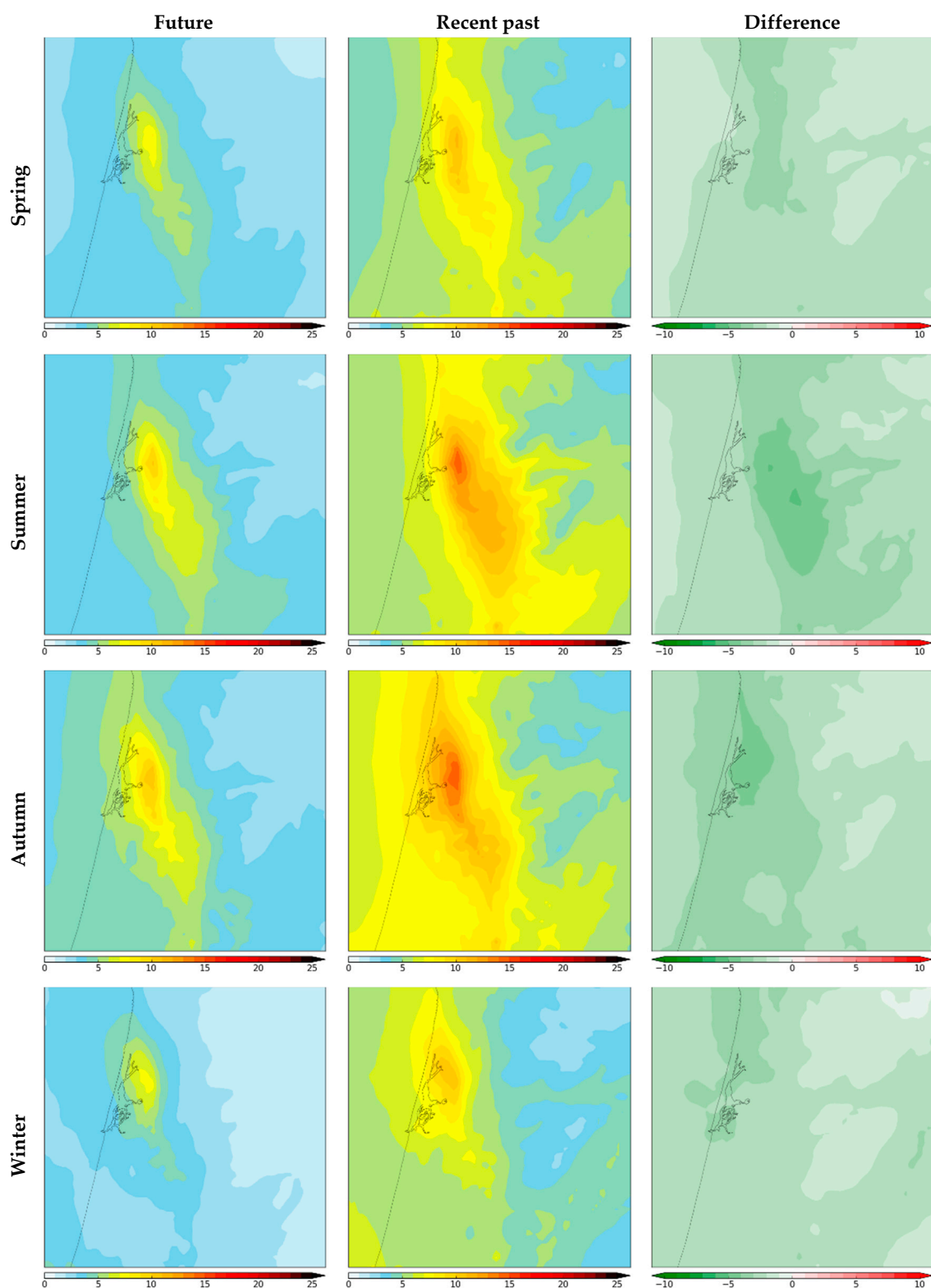
**Figure A5.** Seasonal average concentrations of the maximum daily 8 h mean  $O_3$ , in  $\mu\text{g}\cdot\text{m}^{-3}$ , for the medium-term future climate (2055), recent past climate (2014), and the difference between them (2055–2014). For future and recent past maps, the maximum value of the colour scale represents the EU target value ( $120 \mu\text{g}\cdot\text{m}^{-3}$ ).

Figure A6 shows seasonal average concentrations of PM10, for the medium-term future climate, recent past climate, and the difference between them.



**Figure A6.** Seasonal average concentrations of PM<sub>10</sub>, in  $\mu\text{g}\cdot\text{m}^{-3}$ , for the medium-term future climate (2055), recent past climate (2014), and the difference between them (2055–2014). For future and recent past maps, the maximum value of the colour scale represents the EU limit value ( $40 \mu\text{g}\cdot\text{m}^{-3}$ ).

Figure A7 shows seasonal average concentrations of PM<sub>2.5</sub>, for the medium-term future climate, recent past climate, and the difference between them.



**Figure A7.** Seasonal average concentrations of PM<sub>2.5</sub>, in  $\mu\text{g}\cdot\text{m}^{-3}$ , for the medium-term future climate (2055), recent past climate (2014), and the difference between them (2055–2014). For future and recent past maps, the maximum value of the colour scale represents the EU limit value ( $25 \mu\text{g}\cdot\text{m}^{-3}$ ).

To analyse the quantitative CAMx performance, the following statistical parameters were used: (i) correlation coefficient; (ii) mean bias; (iii) mean error; (iv) index of agreement; (v) root mean square error (RMSE); and (vi) modelling quality indicator (MQI), considering

a deviation between modelled and measured concentrations as twice the measurement uncertainty, as defined by Janssen and Thunis [95]. Table A1 summarizes the values of the CAMx performance statistics, for NO<sub>2</sub>, O<sub>3</sub>, and PM10.

**Table A1.** CAMx performance statistics for NO<sub>2</sub> hourly concentrations, O<sub>3</sub> 8 h mean concentrations, and PM10 daily mean concentrations, computed for the recent past climate (2014), for three air quality monitoring stations (EST—Estarreja, industrial background; ILH—Ílhavo, suburban background; and FRN—Fornelo do Monte, rural background).

	NO <sub>2</sub>			O <sub>3</sub>			PM10		
	EST	ILH	FRN	EST	ILH	FRN	EST	ILH	FRN
Nr <sup>o</sup> Observations [%]	100	97	100	344	356	365	100	99	100
Correlation [-]	0.39	0.32	0.68	0.52	0.50	0.54	0.33	0.54	0.52
Mean Bias [ $\mu\text{g}\cdot\text{m}^{-3}$ ]	−1.56	−0.26	−0.72	1.72	2.50	3.22	−6.79	−1.10	−5.65
Mean Error [ $\mu\text{g}\cdot\text{m}^{-3}$ ]	5.67	0.99	3.76	15.95	12.87	13.93	10.67	3.53	7.10
Index of Agreement [-]	0.62	0.64	0.89	0.70	0.68	0.68	0.73	0.64	0.48
RMSE [ $\mu\text{g}\cdot\text{m}^{-3}$ ]	7.31	1.27	5.24	20.43	16.86	17.36	14.72	5.57	9.18
MQI [-]	0.35	0.07	0.26	0.26	0.21	0.22	0.90	0.93	0.86

For the three air quality stations, mean bias for NO<sub>2</sub>, O<sub>3</sub> and PM10 range from −1.56 to −0.26  $\mu\text{g}\cdot\text{m}^{-3}$ , from 1.72 to 3.22  $\mu\text{g}\cdot\text{m}^{-3}$ , and from −6.79 to −1.10  $\mu\text{g}\cdot\text{m}^{-3}$ , respectively, showing a general underestimation of NO<sub>2</sub> and PM10, and the overestimation of O<sub>3</sub>. Higher RMSE are found for O<sub>3</sub>, with values up to 15.95  $\mu\text{g}\cdot\text{m}^{-3}$  and 20.43  $\mu\text{g}\cdot\text{m}^{-3}$ , respectively. Correlation and index of agreement for the three pollutants cover a range from 0.32 to 0.68. For the modelling quality indicator, values below 1 are obtained for all air quality monitoring stations and pollutants. According to the FAIRMODE guidelines [95], 90th percentile MQI values below 1 indicate that the modelling quality objective, defined as the minimum level of quality to be achieved by a model for policy use, is fulfilled.

The CAMx performance can be attributed to different factors. Some studies [17,100,101] stated that NO<sub>2</sub> and PM10 underestimations could be explained by a potential overestimation of the vertical mixing. Additionally, a potential underestimation/overestimation in the emission inventory database could lead to the CAMx underestimation/overestimation [17,102]. Further, the CAMx performance could also be affected by the WRF meteorological fields. As one of the objectives of this work is to compare future climate results with those of the recent past, the same methodology had to be adopted for both periods. Thus, the WRF simulation was forced by the climate model MPI-ESM and not with data from observations/reanalysis, which may affect the WRF performance, and consequently the CAMx results. Nonetheless, other studies [30–32] evaluated the use of MPI-ESM data as WRF forcing, obtaining a high level of confidence in this model configuration for climate studies.

## References

1. Grossberndt, S.; Bartonova, A.; Ortiz, A.G. *Public Awareness and Efforts to Improve Air Quality in Europe*; Eionet Report-ETC/ATNI 2020/2; European Topic Centre on Air Pollution, Transport, Noise and Industrial Pollution: Kjeller, Norway, 2021.
2. Von Schneidmesser, E.; Monks, P.S.P.S.; Allan, J.D.J.D.; Bruhwiler, L.; Forster, P.; Fowler, D.; Lauer, A.; Morgan, W.T.W.T.; Paasonen, P.; Righi, M.; et al. Chemistry and the Linkages between Air Quality and Climate Change. *Chem. Rev.* **2015**, *115*, 3856–3897. [[CrossRef](#)] [[PubMed](#)]
3. Eurostat. *Urban Europe: Statistics on Cities, Towns and Suburbs—2016 Edition*; Publications Office of the European Union: Luxembourg, 2016.
4. EEA. Exceedance of Air Quality Standards in Europe. Available online: <https://www.eea.europa.eu/ims/exceedance-of-air-quality-standards#footnote-RWRZZSXA> (accessed on 29 August 2022).
5. EC. Directive 2008/50/EC of the European Parliament and of the Council of 21 May 2008 on Ambient Air Quality and Cleaner Air for Europe. *Eur. Comm.-Off. J. Eur. Union* **2008**, *L152*, 1–44.
6. WHO. *Global Air Quality Guidelines: Particulate Matter (PM<sub>2.5</sub> and PM<sub>10</sub>), Ozone, Nitrogen Dioxide, Sulfur Dioxide and Carbon Monoxide*; World Health Organization: Geneva, Switzerland, 2021.

7. EC. *Communication from the Commission to the European Parliament, the Council, the European Economic and Social Committee and the Committee of the Regions—“A Clean Air Programme for Europe”*; European Commission: Brussels, Belgium, 2013.
8. EC. *Communication from the Commission to the European Parliament, the European Council, the Council, the European Economic and Social Committee and the Committee of the Regions—“The European Green Deal”*; European Commission: Brussels, Belgium, 2019.
9. WHO. *World Health Statistics 2022: Monitoring Health for the SDGs, Sustainable Development Goals*; World Health Organization: Geneva, Switzerland, 2022.
10. EEA. *Air Quality in Europe 2021*; Report No. 15/2021; European Environmental Agency: Luxembourg, 2021.
11. Seo, J.; Kim, J.Y.; Youn, D.; Lee, J.Y.; Kim, H.; Lim, Y.B.; Kim, Y.; Jin, H.C. On the Multiday Haze in the Asian Continental Outflow: The Important Role of Synoptic Conditions Combined with Regional and Local Sources. *Atmos. Chem. Phys.* **2017**, *17*, 9311–9332. [[CrossRef](#)]
12. Coelho, S.; Rafael, S.; Lopes, D.; Miranda, A.I.; Ferreira, J. How Changing Climate May Influence Air Pollution Control Strategies for 2030? *Sci. Total Environ.* **2021**, *758*, 143911. [[CrossRef](#)]
13. IPCC. *Climate Change 2021: The Physical Science Basis. Contribution of Working Group I to the Sixth Assessment Report of the Intergovernmental Panel on Climate Change*; Masson-Delmotte, V., Zhai, P., Pirani, A., Connors, S.L., Péan, C., Berger, S., Caud, N., Chen, Y., Goldfarb, L., Gomis, M.I., et al., Eds.; Cambridge University Press: Cambridge, UK, 2021; in press.
14. Revi, A.; Satterthwaite, D.; Aragón-Durand, F.; Corfee-Morlot, J.; Kiunsi, R.B.R.; Pelling, M.; Roberts, D.C.; Solecki, W. Urban Areas. In *Climate Change 2014: Impacts, Adaptation, and Vulnerability. Part A: Global and Sectoral Aspects. Contribution of Working Group II to the Fifth Assessment Report of the Intergovernmental Panel on Climate Change*; Field, C.B., Barros, V.R., Dokken, D.J., Mach, K.J., Mastrandrea, M.D., Bilir, T.E., Chatterjee, M., Ebi, K.L., Estrada, Y.O., Genova, R.C., et al., Eds.; Cambridge University Press: Cambridge, UK; New York, NY, USA, 2014; pp. 535–612. ISBN 9781107415379.
15. Radhakrishnan, M.; Islam, T.; Ashley, R.M.; Pathirana, A.; Quan, N.H.; Gersonius, B.; Zevenbergen, C. Context Specific Adaptation Grammars for Climate Adaptation in Urban Areas. *Environ. Model. Softw.* **2018**, *102*, 73–83. [[CrossRef](#)]
16. Radhakrishnan, M.; Pathirana, A.; Ashley, R.; Zevenbergen, C. Structuring Climate Adaptation through Multiple Perspectives: Framework and Case Study on Flood Risk Management. *Water* **2017**, *9*, 129. [[CrossRef](#)]
17. Coelho, S.; Ferreira, J.; Rodrigues, V.; Lopes, M. Source Apportionment of Air Pollution in European Urban Areas: Lessons from the ClairCity Project. *J. Environ. Manag.* **2022**, *320*, 115899. [[CrossRef](#)]
18. Jiang, Y.; Hou, L.; Shi, T.; Gui, Q. A Review of Urban Planning Research for Climate Change. *Sustainability* **2017**, *9*, 2224. [[CrossRef](#)]
19. Monjardino, J.; Dias, L.; Vale, G.; Tente, H.; Gouveia, J.P.; Barroso, J.E.; Dias, L.; Aires, N.; Fortes, P.; Ferreira, F.; et al. *Relatório Setorial: Estimativa de Poluentes Atmosféricos. Trabalhos de Base Para o Roteiro Para a Neutralidade Carbónica 2050*; UNFCC: Bonn, Germany, 2019.
20. Rodrigues, V.; Gama, C.; Ascenso, A.; Oliveira, K.; Coelho, S.; Monteiro, A.; Hayes, E.; Lopes, M. Assessing Air Pollution in European Cities to Support a Citizen Centered Approach to Air Quality Management. *Sci. Total Environ.* **2021**, *799*, 149311. [[CrossRef](#)]
21. Coelho, S.; Rodrigues, V.; Barnes, J.; Boushel, C.; Devito, L.; Lopes, M. Air Pollution in the Aveiro Region, Portugal: A Citizens' Engagement Approach. *WIT Trans. Ecol. Environ.* **2018**, *230*, 253–262. [[CrossRef](#)]
22. Slingerland, S.; Artola, I.; Lopes, M.; Rodrigues, V.; Borrego, C.; Miranda, A.I.; Silva, S.; Coelho, S.; Cravo, O.; Matos, J.E. *D6.2 Air Quality and Climate Related Policies in the Intermunicipal Community of the Region of Aveiro (CIRA, Portugal)—Baseline Analysis*; CESAM: Rotterdam, The Netherlands, 2018.
23. Peel, M.C.; Finlayson, B.L.; McMahon, T.A. Updated World Map of the Köppen-Geiger Climate Classification. *Hydrol. Earth Syst. Sci.* **2007**, *11*, 1633–1644. [[CrossRef](#)]
24. Skamarock, W.C.; Klemp, J.B.; Dudhia, J.; Gill, D.O.; Liu, Z.; Berner, J.; Wang, W.; Powers, J.G.; Duda, M.G.; Barker, D.M.; et al. *A Description of the Advanced Research WRF Version 4*. NCAR Tech. Note NCAR/TN-556+STR; UCAR: Boulder, CO, USA, 2019.
25. ENVIRON CAMx. *User's Guide. Comprehensive Air Quality Model with Extensions. Version 7.10*; Ramboll Environment and Health: Arlington, VA, USA, 2020.
26. Ferreira, J.; Lopes, D.; Rafael, S.; Relvas, H.; Almeida, S.M.; Miranda, A.I. Modelling Air Quality Levels of Regulated Metals: Limitations and Challenges. *Environ. Sci. Pollut. Res.* **2020**, *27*, 33916–33928. [[CrossRef](#)] [[PubMed](#)]
27. Rafael, S.; Martins, H.; Marta-Almeida, M.; Sá, E.; Coelho, S.; Rocha, A.; Borrego, C.; Lopes, M. Quantification and Mapping of Urban Fluxes under Climate Change: Application of WRF-SUEWS Model to Greater Porto Area (Portugal). *Environ. Res.* **2017**, *155*, 321–334. [[CrossRef](#)] [[PubMed](#)]
28. Mauritsen, T.; Bader, J.; Becker, T.; Behrens, J.; Bittner, M.; Brokopf, R.; Brovkin, V.; Claussen, M.; Crueger, T.; Esch, M.; et al. Developments in the MPI-M Earth System Model Version 1.2 (MPI-ESM1.2) and Its Response to Increasing CO<sub>2</sub>. *J. Adv. Model. Earth Syst.* **2019**, *11*, 998–1038. [[CrossRef](#)]
29. Brands, S.; Herrera, S.; Fernández, J.; Gutiérrez, J.M. How Well Do CMIP5 Earth System Models Simulate Present Climate Conditions in Europe and Africa? *Clim. Dyn.* **2013**, *41*, 803–817. [[CrossRef](#)]
30. Marta-Almeida, M.; Teixeira, J.C.; Carvalho, M.J.; Melo-Gonçalves, P.; Rocha, A.M. High Resolution WRF Climatic Simulations for the Iberian Peninsula: Model Validation. *Phys. Chem. Earth, Parts A/B/C* **2016**, *94*, 94–105. [[CrossRef](#)]
31. Rafael, S.; Martins, H.; Matos, M.J.; Cerqueira, M.; Pio, C.; Lopes, M.; Borrego, C. Application of SUEWS Model Forced with WRF: Energy Fluxes Validation in Urban and Suburban Portuguese Areas. *Urban Clim.* **2020**, *33*, 100662. [[CrossRef](#)]

32. Russo, M.A.; Carvalho, D.; Martins, N.; Monteiro, A. Future Perspectives for Wind and Solar Energy Production in Portugal under High-Resolution Climate Change Scenarios. *Renew. Sustain. Energy Rev.* 2022; under review. 2022.
33. Coelho, S.; Rafael, S.; Coutinho, M.; Monteiro, A.; Medina, J.; Figueiredo, S.; Cunha, S.; Lopes, M.; Miranda, A.I.A.I.; Borrego, C. Climate-Change Adaptation Framework for Multiple Urban Areas in Northern Portugal. *Environ. Manag.* **2020**, *66*, 1–12. [[CrossRef](#)]
34. Coelho, S.; Rafael, S.; Fernandes, A.P.; Lopes, M.; Carvalho, D. How the New Climate Scenarios Will Affect Air Quality Trends: An Exploratory Research. *Urban Clim.* under review.
35. Hong, S.; Lim, S. The WRF Single-Moment 6-Class Microphysics Scheme (WSM6). *J. Korean Meteorol. Soc.* **2006**, *42*, 129–151.
36. Iacono, M.J.; Delamere, J.S.; Mlawer, E.J.; Shephard, M.W.; Clough, S.A.; Collins, W.D. Radiative Forcing by Long-Lived Greenhouse Gases: Calculations with the AER Radiative Transfer Models. *J. Geophys. Res.* **2008**, *113*, D13103. [[CrossRef](#)]
37. Jiménez, P.A.; Dudhia, J.; González-Rouco, J.F.; Navarro, J.; Montávez, J.P.; García-Bustamante, E. A Revised Scheme for the WRF Surface Layer Formulation. *Mon. Weather Rev.* **2012**, *140*, 898–918. [[CrossRef](#)]
38. Tewari, M.; Chen, F.; Wang, W.; Dudhia, J.; LeMone, M.A.A.; Mitchell, K.; Ek, M.; Gayno, G.; Wegiel, J.; Cuenca, R.; et al. Implementation and Verification of the Unified NOAA Land Surface Model in the WRF Model. In Proceedings of the 20th Conference on Weather Analysis and Forecasting/16th Conference on Numerical Weather Prediction, Seattle, WA, USA, 12–16 January 2004; pp. 11–15.
39. Hong, S.-Y.; Noh, Y.; Dudhia, J. A New Vertical Diffusion Package with an Explicit Treatment of Entrainment Processes. *Mon. Weather Rev.* **2006**, *134*, 2318–2341. [[CrossRef](#)]
40. Grell, G.A.; Freitas, S.R. A Scale and Aerosol Aware Stochastic Convective Parameterization for Weather and Air Quality Modeling. *Atmos. Chem. Phys.* **2014**, *14*, 5233–5250. [[CrossRef](#)]
41. Ascenso, A.; Augusto, B.; Silveira, C.; Rafael, S.; Coelho, S.; Monteiro, A.; Ferreira, J.; Menezes, I.; Roebeling, P.; Miranda, A.I. Impacts of Nature-Based Solutions on the Urban Atmospheric Environment: A Case Study for Eindhoven, The Netherlands. *Urban For. Urban Green.* **2021**, *57*, 126870. [[CrossRef](#)]
42. Wang, X.Y.; Wang, K.C. Estimation of Atmospheric Mixing Layer Height from Radiosonde Data. *Atmos. Meas. Tech.* **2014**, *7*, 1701–1709. [[CrossRef](#)]
43. Kayes, I.; Shahriar, S.A.; Hasan, K.; Akhter, M.; Kabir, M.M.; Salam, M.A. The Relationships between Meteorological Parameters and Air Pollutants in an Urban Environment. *Glob. J. Environ. Sci. Manag.* **2019**, *5*, 265–278. [[CrossRef](#)]
44. Aw, J.; Kleeman, M.J. Evaluating the First-Order Effect of Intraannual Temperature Variability on Urban Air Pollution. *J. Geophys. Res. Atmos.* **2003**, *108*, 688. [[CrossRef](#)]
45. Jacob, D.J.; Winner, D.A. Effect of Climate Change on Air Quality. *Atmos. Environ.* **2009**, *43*, 51–63. [[CrossRef](#)]
46. Fricko, O.; Havlik, P.; Rogelj, J.; Klimont, Z.; Gusti, M.; Johnson, N.; Kolp, P.; Strubegger, M.; Valin, H.; Amann, M.; et al. The Marker Quantification of the Shared Socioeconomic Pathway 2: A Middle-of-the-Road Scenario for the 21st Century. *Glob. Environ. Chang.* **2017**, *42*, 251–267. [[CrossRef](#)]
47. Riahi, K.; van Vuuren, D.P.; Kriegler, E.; Edmonds, J.; O'Neill, B.C.; Fujimori, S.; Bauer, N.; Calvin, K.; Dellink, R.; Fricko, O.; et al. The Shared Socioeconomic Pathways and Their Energy, Land Use, and Greenhouse Gas Emissions Implications: An Overview. *Glob. Environ. Chang.* **2017**, *42*, 153–168. [[CrossRef](#)]
48. Emmons, L.K.; Schwantes, R.H.; Orlando, J.J.; Tyndall, G.; Kinnison, D.; Lamarque, J.-F.; Marsh, D.; Mills, M.J.; Tilmes, S.; Bardeen, C.; et al. The Chemistry Mechanism in the Community Earth System Model Version 2 (CESM2). *J. Adv. Model. Earth Syst.* **2020**, *12*, e2019MS001882. [[CrossRef](#)]
49. EMEP. European Monitoring and Evaluation Programme. Available online: <http://www.emep.int/> (accessed on 21 March 2022).
50. Yarwood, G.; Jung, J.; Whitten, G.Z.; Heo, G.; Mellberg, J.; Estes, M. Updates to the Carbon Bond Mechanism for Version 6 (CB6). In Proceedings of the 9th Annual CMAS Conference, Chapel Hill, NC, USA, 11–13 October 2010.
51. Sá, E.; Ferreira, J.; Carvalho, A.; Borrego, C. Development of Current and Future Pollutant Emissions for Portugal. *Atmos. Pollut. Res.* **2015**, *6*, 849–857. [[CrossRef](#)]
52. WHO. *Review of Evidence on Health Aspects of Air Pollution—REVIHAAP Project*; Technical Report; World Health Organization: Copenhagen, Denmark, 2013.
53. Amnuaylojaroen, T.; Parasin, N.; Limsakul, A. Health Risk Assessment of Exposure Near-Future PM2.5 in Northern Thailand. *Air Qual. Atmos. Health* **2022**, 1–17. [[CrossRef](#)]
54. Brook, R.D.; Rajagopalan, S.; Pope, C.A.; Brook, J.R.; Bhatnagar, A.; Diez-Roux, A.V.; Holguin, F.; Hong, Y.; Luepker, R.V.; Mittleman, M.A.; et al. Particulate Matter Air Pollution and Cardiovascular Disease: An Update to the Scientific Statement from the American Heart Association. *Circulation* **2010**, *121*, 2331–2378. [[CrossRef](#)] [[PubMed](#)]
55. Næss, Ø.; Nafstad, P.; Aamodt, G.; Clausen, B.; Rosland, P. Relation between Concentration of Air Pollution and Cause-Specific Mortality: Four-Year Exposures to Nitrogen Dioxide and Particulate Matter Pollutants in 470 Neighborhoods in Oslo, Norway. *Am. J. Epidemiol.* **2007**, *165*, 435–443. [[CrossRef](#)] [[PubMed](#)]
56. Marmett, B.; Carvalho, R.B.; Nunes, R.B.; Rhoden, C.R. Exposure to O<sub>3</sub> and NO<sub>2</sub> in Physically Active Adults: An Evaluation of Physiological Parameters and Health Risk Assessment. *Environ. Geochem. Health* **2022**, 1–16. [[CrossRef](#)]
57. Brunekreef, B. Health Effects of Air Pollution Observed in Cohort Studies in Europe. *J. Expo. Sci. Environ. Epidemiol.* **2007**, *17*, S61–S65. [[CrossRef](#)]

58. Cesaroni, G.; Badaloni, C.; Gariazzo, C.; Stafoggia, M.; Sozzi, R.; Davoli, M.; Forastiere, F. Long-Term Exposure to Urban Air Pollution and Mortality in a Cohort of More than a Million Adults in Rome. *Environ. Health Perspect.* **2013**, *121*, 324–331. [[CrossRef](#)]
59. Soares, A.R.; Silva, C. Review of Ground-Level Ozone Impact in Respiratory Health Deterioration for the Past Two Decades. *Atmosphere* **2022**, *13*, 434. [[CrossRef](#)]
60. Lipfert, F.W.; Wyzga, R.E.; Baty, J.D.; Miller, J.P. Traffic density as a surrogate measure of environmental exposures in studies of air pollution health effects: Long-term mortality in a cohort of US veterans. *Atmos. Environ.* **2006**, *40*, 154–169. [[CrossRef](#)]
61. Soares, J.; Horálek, J.; Ortiz, A.G.; Guerreiro, C.; Gsella, A. *Health Risk Assessment of Air Pollution in Europe. Methodology Description and 2017 Results*; ETC/ATNI Report 13/2019; European Topic Centre on Air Pollution, Transport, Noise and Industrial Pollution: Kjeller, Norway, 2019.
62. EEA. *Assessing the Risks to Health from Air Pollution*; Briefing No. 11/2018; European Environment Agency: Copenhagen, Denmark, 2018.
63. WHO. *Health Risk Assessment of Air Pollution—General Principles*; World Health Organization: Copenhagen, Denmark, 2016.
64. INE. Resident Population (No.) by Place of Residence, Sex and Age Group; Decennial—Statistics Portugal, Population and Housing Census—2021. Available online: [https://www.ine.pt/xportal/xmain?xpid=INE&xpgid=ine\\_indicadores&indOcorrCod=0011166&contexto=bd&selTab=tab2](https://www.ine.pt/xportal/xmain?xpid=INE&xpgid=ine_indicadores&indOcorrCod=0011166&contexto=bd&selTab=tab2) (accessed on 28 July 2022).
65. INE. Resident Population (Projections 2015–2080—No.) by Place of Residence (NUTS—2013), Sex, Age and Scenario; Annual—Statistics Portugal, Resident Population Projections. Available online: [https://www.ine.pt/xportal/xmain?xpid=INE&xpgid=ine\\_indicadores&indOcorrCod=0009098&contexto=bd&selTab=tab2](https://www.ine.pt/xportal/xmain?xpid=INE&xpgid=ine_indicadores&indOcorrCod=0009098&contexto=bd&selTab=tab2) (accessed on 28 July 2022).
66. WHO. *Health Risks of Air Pollution in Europe—HRAPIE Project: Recommendations for Concentration–Response Functions for Cost–Benefit Analysis of Particulate Matter, Ozone and Nitrogen Dioxide*; World Health Organization: Copenhagen, Denmark, 2013.
67. Jerrett, M.; Burnett, R.T.; Pope, C.A.; Ito, K.; Thurston, G.; Krewski, D.; Shi, Y.; Calle, E.; Thun, M. Long-Term Ozone Exposure and Mortality. *N. Engl. J. Med.* **2009**, *360*, 1085–1095. [[CrossRef](#)] [[PubMed](#)]
68. Hoek, G.; Krishnan, R.M.; Beelen, R.; Peters, A.; Ostro, B.; Brunekreef, B.; Kaufman, J.D. Long-Term Air Pollution Exposure and Cardio-Respiratory Mortality: A Review. *Environ. Health A Glob. Access Sci. Source* **2013**, *12*, 1–16. [[CrossRef](#)] [[PubMed](#)]
69. Chen, J.; Hoek, G. Long-Term Exposure to PM and All-Cause and Cause-Specific Mortality: A Systematic Review and Meta-Analysis. *Environ. Int.* **2020**, *143*, 105974. [[CrossRef](#)] [[PubMed](#)]
70. Huangfu, P.; Atkinson, R. Long-Term Exposure to NO<sub>2</sub> and O<sub>3</sub> and All-Cause and Respiratory Mortality: A Systematic Review and Meta-Analysis. *Environ. Int.* **2020**, *144*, 105998. [[CrossRef](#)] [[PubMed](#)]
71. Weichenthal, S.; Villeneuve, P.J.; Burnett, R.T.; van Donkelaar, A.; Martin, R.V.; Jones, R.R.; DellaValle, C.T.; Sandler, D.P.; Ward, M.H.; Hoppin, J.A. Long-Term Exposure to Fine Particulate Matter: Association with Nonaccidental and Cardiovascular Mortality in the Agricultural Health Study Cohort. *Environ. Health Perspect.* **2014**, *122*, 609–615. [[CrossRef](#)] [[PubMed](#)]
72. Pinault, L.; Tjepkema, M.; Crouse, D.L.; Weichenthal, S.; Van Donkelaar, A.; Martin, R.V.; Brauer, M.; Chen, H.; Burnett, R.T. Risk Estimates of Mortality Attributed to Low Concentrations of Ambient Fine Particulate Matter in the Canadian Community Health Survey Cohort. *Environ. Health A Glob. Access Sci. Source* **2016**, *15*, 1–15. [[CrossRef](#)]
73. Pinault, L.L.; Weichenthal, S.; Crouse, D.L.; Brauer, M.; Erickson, A.; van Donkelaar, A.; Martin, R.V.; Hystad, P.; Chen, H.; Finès, P.; et al. Associations between Fine Particulate Matter and Mortality in the 2001 Canadian Census Health and Environment Cohort. *Environ. Res.* **2017**, *159*, 406–415. [[CrossRef](#)]
74. Cakmak, S.; Hebborn, C.; Pinault, L.; Lavigne, E.; Vanos, J.; Crouse, D.L.; Tjepkema, M. Associations between Long-Term PM 2.5 and Ozone Exposure and Mortality in the Canadian Census Health and Environment Cohort (CANHEC), by Spatial Synoptic Classification Zone. *Environ. Int.* **2018**, *111*, 200–211. [[CrossRef](#)]
75. Villeneuve, P.J.; Weichenthal, S.A.; Crouse, D.; Miller, A.B.; To, T.; Martin, R.V.; Van Donkelaar, A.; Wall, C.; Burnett, R.T. Long-Term Exposure to Fine Particulate Matter Air Pollution and Mortality among Canadian Women. *Epidemiology* **2015**, *26*, 536–545. [[CrossRef](#)]
76. Tonne, C.; Wilkinson, P. Long-Term Exposure to Air Pollution Is Associated with Survival Following Acute Coronary Syndrome. *Eur. Heart J.* **2013**, *34*, 1306–1311. [[CrossRef](#)]
77. Turner, M.C.; Jerrett, M.; Pope, C.A.; Krewski, D.; Gapstur, S.M.; Diver, W.R.; Beckerman, B.S.; Marshall, J.D.; Su, J.; Crouse, D.L.; et al. Long-Term Ozone Exposure and Mortality in a Large Prospective Study. *Am. J. Respir. Crit. Care Med.* **2016**, *193*, 1134–1142. [[CrossRef](#)] [[PubMed](#)]
78. Hart, J.E.; Rimm, E.B.; Rexrode, K.M.; Laden, F. Changes in Traffic Exposure and the Risk of Incident Myocardial Infarction and All-Cause Mortality. *Epidemiology* **2013**, *24*, 734–742. [[CrossRef](#)]
79. Carey, I.M.; Atkinson, R.W.; Kent, A.J.; Van Staa, T.; Cook, D.G.; Anderson, H.R. Mortality Associations with Long-Term Exposure to Outdoor Air Pollution in a National English Cohort. *Am. J. Respir. Crit. Care Med.* **2013**, *187*, 1226–1233. [[CrossRef](#)]
80. Hart, J.E.; Garshick, E.; Dockery, D.W.; Smith, T.J.; Ryan, L.; Laden, F. Long-Term Ambient Multipollutant Exposures and Mortality. *Am. J. Respir. Crit. Care Med.* **2011**, *183*, 73–78. [[CrossRef](#)] [[PubMed](#)]
81. WHO. WHO Mortality Database. Available online: <https://www.who.int/data/data-collection-tools/who-mortality-database> (accessed on 28 May 2022).
82. Murray, C.J.L. Rethinking DALYs. In *The Global Burden of Disease*; Murray, C.J.L., Lopez, A.D., Eds.; Harvard University Press: Cambridge, UK, 1996; pp. 1–98.

83. Vicente-Serrano, S.M.; Lopez-Moreno, J.-I.; Beguería, S.; Lorenzo-Lacruz, J.; Sanchez-Lorenzo, A.; García-Ruiz, J.M.; Azorin-Molina, C.; Morán-Tejeda, E.; Revuelto, J.; Trigo, R.; et al. Evidence of Increasing Drought Severity Caused by Temperature Rise in Southern Europe. *Environ. Res. Lett.* **2014**, *9*, 044001. [[CrossRef](#)]
84. Jacob, D.; Petersen, J.; Eggert, B.; Alias, A.; Christensen, O.B.; Bouwer, L.M.; Braun, A.; Colette, A.; Déqué, M.; Georgievski, G.; et al. EURO-CORDEX: New High-Resolution Climate Change Projections for European Impact Research. *Reg. Environ. Chang.* **2014**, *14*, 563–578. [[CrossRef](#)]
85. MedECC. *Climate and Environmental Change in the Mediterranean Basin—Current Situation and Risks for the Future*; First Mediterranean Assessment Report; Cramer, W., Guiot, J., Marini, K., Eds.; Union for the Mediterranean, Plan Bleu, UNEP/MAP: Marseille, France, 2020; ISBN 978-2-9577416-0-1.
86. Duhanyan, N.; Roustan, Y. Below-Cloud Scavenging by Rain of Atmospheric Gases and Particulates. *Atmos. Environ.* **2011**, *45*, 7201–7217. [[CrossRef](#)]
87. Guo, L.-C.; Zhang, Y.; Lin, H.; Zeng, W.; Liu, T.; Xiao, J.; Rutherford, S.; You, J.; Ma, W. The Washout Effects of Rainfall on Atmospheric Particulate Pollution in Two Chinese Cities. *Environ. Pollut.* **2016**, *215*, 195–202. [[CrossRef](#)]
88. Coelho, S.; Ferreira, J.; Carvalho, D.; Miranda, A.I.; Lopes, M. Climate Change Impact on Source Contributions to the Air Quality in Aveiro Region. In *Air Pollution Modeling and its Application XXVIII, Proceedings of the ITM 2021, Barcelona, Spain, 18–22 October 2021*; Springer Proceedings in Complexity; Mensink, C., Jorba, O., Eds.; Springer International Publishing: Cham, Switzerland, 2023; p. 308.
89. Coelho, S.; Ferreira, J.; Carvalho, D.; Miranda, A.I.; Lopes, M. Air Quality Impacts on Human Health, under a Climate Change Scenario: The Aveiro Region Case Study. In *Proceedings of the 21st International Conference on Harmonisation within Atmospheric Dispersion Modelling for Regulatory Purposes, Aveiro, Portugal, 27–30 September 2022*; Trini-Castelli, S., Miranda, A.I., Augusto, B., Ferreira, J., Eds.; Universidade de Aveiro: Aveiro, Portugal, 2022; pp. 409–414.
90. Sá, E.; Martins, H.; Ferreira, J.; Marta-Almeida, M.; Rocha, A.; Carvalho, A.; Freitas, S.; Borrego, C. Climate Change and Pollutant Emissions Impacts on Air Quality in 2050 over Portugal. *Atmos. Environ.* **2016**, *131*, 209–224. [[CrossRef](#)]
91. Lacressonnière, G.; Peuch, V.-H.H.; Vautard, R.; Arteta, J.; Déqué, M.; Joly, M.; Josse, B.; Marécal, V.; Saint-Martin, D. European Air Quality in the 2030s and 2050s: Impacts of Global and Regional Emission Trends and of Climate Change. *Atmos. Environ.* **2014**, *92*, 348–358. [[CrossRef](#)]
92. Markakis, K.; Valari, M.; Colette, A.; Sanchez, O.; Perrussel, O.; Honore, C.; Vautard, R.; Klimont, Z.; Rao, S. Air Quality in the Mid-21st Century for the City of Paris under Two Climate Scenarios; From the Regional to Local Scale. *Atmos. Chem. Phys.* **2014**, *14*, 7323–7340. [[CrossRef](#)]
93. Markakis, K.; Valari, M.; Engardt, M.; Lacressonnière, G.; Vautard, R.; Andersson, C. Mid-21st Century Air Quality at the Urban Scale under the Influence of Changed Climate and Emissions—Case Studies for Paris and Stockholm. *Atmos. Chem. Phys.* **2016**, *16*, 1877–1894. [[CrossRef](#)]
94. EEA. *Air Quality E-Reporting (AQ e-Reporting)*; European Environmental Agency: Copenhagen, Denmark, 2019.
95. Janssen, S.; Thunis, P. *FAIRMODE Guidance Document on Modelling Quality Objectives and Benchmarking (Version 3.3)*; EUR 31068 EN; Publications Office of the European Union: Luxembourg, 2022.
96. EEA. *Air Quality in Europe: 2017 Report*; Report No. 13/2017; European Environment Agency: Luxembourg, 2017.
97. Silva, R.A.; West, J.J.; Lamarque, J.-F.; Shindell, D.T.; Collins, W.J.; Dalsoren, S.; Faluvegi, G.; Folberth, G.; Horowitz, L.W.; Nagashima, T.; et al. The Effect of Future Ambient Air Pollution on Human Premature Mortality to 2100 Using Output from the ACCMIP Model Ensemble. *Atmos. Chem. Phys.* **2016**, *16*, 9847–9862. [[CrossRef](#)] [[PubMed](#)]
98. Partanen, A.-I.; Landry, J.-S.; Matthews, H.D. Climate and Health Implications of Future Aerosol Emission Scenarios. *Environ. Res. Lett.* **2018**, *13*, 024028. [[CrossRef](#)]
99. Likhvar, V.N.; Pascal, M.; Markakis, K.; Colette, A.; Hauglustaine, D.; Valari, M.; Klimont, Z.; Medina, S.; Kinney, P. A Multi-Scale Health Impact Assessment of Air Pollution over the 21st Century. *Sci. Total Environ.* **2015**, *514*, 439–449. [[CrossRef](#)] [[PubMed](#)]
100. Pepe, N.; Pirovano, G.; Lonati, G.; Balzarini, A.; Toppetti, A.; Riva, G.M.; Bedogni, M. Development and Application of a High-Resolution Hybrid Modelling System for the Evaluation of Urban Air Quality. *Atmos. Environ.* **2016**, *141*, 297–311. [[CrossRef](#)]
101. Emery, C.; Tai, E.; Yarwood, G.; Morris, R. Investigation into Approaches to Reduce Excessive Vertical Transport over Complex Terrain in a Regional Photochemical Grid Model. *Atmos. Environ.* **2011**, *45*, 7341–7351. [[CrossRef](#)]
102. Oikonomakis, E.; Aksoyoglu, S.; Ciarelli, G.; Baltensperger, U.; Prévôt, A.S.H. Low Modeled Ozone Production Suggests Underestimation of Precursor Emissions (Especially NO<sub>x</sub>) in Europe. *Atmos. Chem. Phys.* **2018**, *18*, 2175–2198. [[CrossRef](#)]